On the use of perfectly matched layers in the presence of long or backward propagating guided elastic waves

Anne-Sophie Bonnet-Ben Dhia, Colin Chambeyron, Guillaume Legendre

▶ **To cite this version:**

Anne-Sophie Bonnet-Ben Dhia, Colin Chambeyron, Guillaume Legendre. On the use of perfectly matched layers in the presence of long or backward propagating guided elastic waves. Wave Motion, 2014, 51 (2), pp.266-283. 10.1016/j.wavemoti.2013.08.001 . hal-00816895v2

HAL Id: hal-00816895
https://hal.science/hal-00816895v2

Submitted on 18 Jul 2013

HAL is a multi-disciplinary open access archive for the deposit and dissemination of scientific research documents, whether they are published or not. The documents may come from teaching and research institutions in France or abroad, or from public or private research centers.

L'archive ouverte pluridisciplinaire **HAL**, est destinée au dépôt et à la diffusion de documents scientifiques de niveau recherche, publiés ou non, émanant des établissements d'enseignement et de recherche français ou étrangers, des laboratoires publics ou privés.

On the use of perfectly matched layers in the presence of long or backward propagating guided elastic waves

Anne-Sophie Bonnet-Ben Dhia, Colin Chambeyron, Guillaume Legendre

July 18, 2013

Abstract

An efficient method to compute the scattering of a guided wave by a localized defect, in an elastic waveguide of infinite extent and bounded cross section, is considered. It relies on the use of perfectly matched layers (PML) to reduce the problem to a bounded portion of the guide, allowing for a classical finite element discretization. The difficulty here comes from the existence of backward propagating modes, which are not correctly handled by the PML. We propose a simple strategy, based on finite-dimensional linear algebra arguments and using the knowledge of the modes, to recover a correct approximation to the solution with a low additional cost compared to the standard PML approach. Numerical experiments are presented in the two-dimensional case involving Rayleigh–Lamb modes.

1 Introduction

Since their introduction by Bérenger [1], the perfectly matched layers (PML) have been applied to a large number of time-dependent and time-harmonic wave-equation problems set on unbounded domains. For such problems, it is necessary, if any computation is to be done, to put artificial boundaries at some distance away from the given region of interest and, in order to give accurate and reliable results, this truncation has to produce an error on the solution as small as possible. The PML provide a way to do so by introducing layers surrounding the domain of interest in which the waves enter without reflection and decay exponentially, hence solving the difficult task of choosing an adequate boundary condition at the end of the computational domain. Moreover, they are relatively easy to implement in conjunction with virtually any conventional approximation method, like the finite difference, finite element or spectral methods, and can be adapted to solve problems originating from electromagnetism, acoustics, or elasticity, to name a few. They are also generally very efficient and often compare favorably with other existing techniques for artificially handling unbounded domains (see for instance the reference [2], in which a comparison of the performances of high-order absorbing boundary conditions and several types of perfectly matched layers in two dimensions, for problems governed by the Helmholtz equation, is offered).

Despite this undeniable success, the PML technique has been shown to fail in some specific situations. For linear elastic systems in which the propagative medium presents particular anisotropy properties, numerical instabilities can be observed in time-domain simulations [3]. In the context of waveguides, anisotropy of the material is not even a necessary feature for this phenomenon to occur. Investigations connected this behavior to the existence of so-called *backward waves*, whose group and phase velocities have opposite signs.[1] In their presence, exponentional growth occurs in the layers, rendering the method completely unusable [8, 9]. While the generated instabilities are largely discernible in transient simulations, it should be emphasized that it is not the case in time-harmonic ones, the solution effectively computed, usually in a numerically stable manner, simply being not an approximation to the *outgoing* solution of the problem. Additionally, one should mention that the PML also perform very poorly when so-called *long waves* (associated with a mode which has an almost zero propagation constant) arise near cut-off frequencies, as the slow decay of these in the PML region calls for a very thick layer (and thus expensive computations in practice).

In the present article, we are interested by the numerical solution of time-harmonic problems set in (semi-)infinite waveguides. We introduce an original methodology based on a previous idea (see [10]), which can be

[1] The possibility of their existence having been first discussed by Lamb [4], it is now well-known that such waves are present in linear elasticity (see [5] for instance), as the inspection of the dispersion curves of Rayleigh–Lamb modes for some homogeneous, isotropic elastic plates shows that, for a majority of commonly encountered materials and in some frequency ranges, the phase and the energy of a given mode can propagate in opposite directions. These "backward-waves" modes also appear in dielectric-loaded circular electromagnetic waveguides, as discovered in [6], or in layered elastic structures (see [7]).

seen as a way to rehabilitate the use of PML in the presence of backward waves and/or a means to improve its performance when long waves exist, at a moderate additional computational cost. It makes essential use of the orthogonality (or biorthogonality) properties enjoyed by the guided modes and the *a priori* knowledge that some of these modes are associated with backward and/or long waves. It therefore bears some strong similarities with the method proposed by Skelton *et al.* in [8] to overcome the very same issue, which uses the biorthogonality relations satisfied by the Rayleigh–Lamb modes to separate the forward propagating waves from the backward ones in order to treat them appropriately within the PML. It also shares a bond with the approach proposed by Barnett and Greengard in [11] for an integral representation for quasi-periodic scattering problems, in the sense that it involves the computation of a finite number of "corrections", which measure in some way the failure of the approximate solution to satisfy a radiation condition.

Our presentation will be focused on the case of an elastic waveguide, which is particularly interesting as the potential applications are numerous, notably for the detection of cracks within plates, rods, or pipes, in nondestructive testing, but the underlying idea is quite general and can be applied to other wave propagation models. Note however that, due to pending open theoretical questions on modal expansion series of guided elastic modes, we were not able to give a rigorous mathematical justification of the method, as we achieved in [10] with the same technique applied to the use of Robin-type boundary conditions as approximate radiation condition at finite distance for the Helmholtz equation. As a consequence, several essential facts need to be assumed or conjectured for the method to be applicable in the present context.

Our paper is organized as follows. In section 2, the general setting of the problem is given and the modal formalism to be used throughout is recalled. The PML technique and its drawbacks are described in section 3 and the novel methodology is presented in section 4. Details on its implementation are provided in section 5 and a few numerical results are shown in the following section. Finally, we address in the closing section some mathematical questions concerning this work which, to the best of our knowledge, remain open.

2 General setting

In this paper, the elastic wave propagation problems we aim at solving numerically can be either radiation or scattering problems, in which one wants to determine respectively the field generated by a compactly supported source placed in the waveguide or the scattered field due to a local perturbation of the waveguide given an incident field at infinity. The present section is devoted to their mathematical modeling and properties.

2.1 The elastic waveguide

For the sake of simplicity, we consider an isotropic elastic waveguide of semi-infinite length, an extension to the infinite case being dealt with in section 5. Let $\Omega \subset \mathbb{R}^d$, with $d = 2$ or 3, be a connected unbounded domain, obtained by locally perturbing the perfectly straight waveguide, whose cross section S is a bounded subset of $\mathbb{R}^{d-1}$. More precisely, suppose that $\Omega \cap \{\boldsymbol{x} = (\boldsymbol{x}_S, x_d) \,|\, x_d > 0\} = \Omega_+$, and $\Omega \cap \{\boldsymbol{x} = (\boldsymbol{x}_S, x_d) \,|\, x_d < 0\} = \Omega_0$ is a bounded domain possibly containing a localized perturbation of the cylindrical geometry of the waveguide, either a deformation of the boundary or a defect (a crack for instance) enclosed in the guide (see Figure 1 for an example).

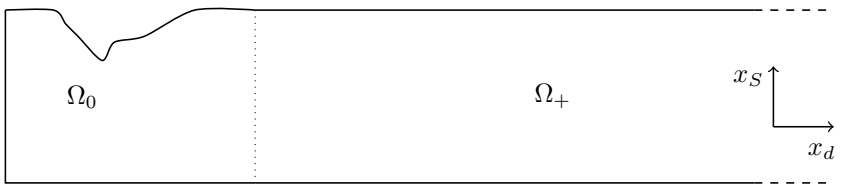

Figure 1: A realization of the domain Ω in two dimensions, representing a waveguide of semi-infinite length with a local boundary deformation.

Within the framework of linear elasticity theory, a time-harmonic dependence of pulsation $\omega > 0$ being assumed, the (vectorial) displacement is the quantity $\mathrm{Re}(\boldsymbol{u}(\boldsymbol{x})\, e^{-\mathrm{i}\omega\, t})$, where the field $\boldsymbol{u}$ satisfies the following equations (note that the $e^{-\mathrm{i}\omega\, t}$ factor will be omitted henceforth)

$$-\rho\omega^2 \boldsymbol{u} - \mathrm{div}(\boldsymbol{\sigma}(\boldsymbol{u})) = \boldsymbol{f} \text{ in } \Omega, \tag{1}$$

with the stress-free boundary condition

$$\boldsymbol{\sigma}(\boldsymbol{u})\boldsymbol{n} = \boldsymbol{0} \text{ on } \partial\Omega, \tag{2}$$

in which ρ is the mass density of the material forming the waveguide, $\boldsymbol{\sigma}(\boldsymbol{u})$ is the stress tensor, $\boldsymbol{f}$ is a source term with compact support in Ω_0 and $\boldsymbol{n}$ is the unit outward normal vector to $\partial\Omega$, the boundary of Ω. In order to close the system (1)-(2), one must prescribe the relationship between the stress tensor and the strain tensor $\boldsymbol{\varepsilon}(\boldsymbol{u}) = \frac{1}{2}\left(\boldsymbol{\nabla u} + (\boldsymbol{\nabla u})^T\right)$, which is done by Hooke's law

$$\boldsymbol{\sigma}(\boldsymbol{u}) = \lambda\, \mathrm{div}(\boldsymbol{u})\, \mathbf{I} + 2\mu\, \boldsymbol{\varepsilon}(\boldsymbol{u}), \tag{3}$$

where λ and μ are the Lamé parameters, given by

$$\lambda = \frac{E\nu}{(1+\nu)(1-2\nu)} \text{ and } \mu = \frac{E}{2(1+\nu)},$$

with E and ν the Young modulus and the Poisson ratio of the elastic material.

2.2 Guided elastic modes and biorthogonality

An essential tool used throughout these pages is the modal series expansion of the solution to the elastic wave propagation problem in the unperturbed straight part of the waveguide. In order to make the present article more self-contained, let us collect some basic but fundamental notions and properties relative to guided elastic modes.

The modes of the waveguide are solutions with separated variables of the standard form

$$\boldsymbol{u}(\boldsymbol{x}) = \mathbf{u}(\boldsymbol{x}_S)\, e^{\mathrm{i}\beta x_d},$$

where the function $\mathbf{u}$ and the complex number β are respectively the field profile and the propagation constant of the mode, to the system of homogeneous equations

$$\begin{aligned} &-\rho\omega^2\boldsymbol{u} - \mathrm{div}(\boldsymbol{\sigma}(\boldsymbol{u})) = \mathbf{0} \text{ in } S\times\mathbb{R},\\ &\boldsymbol{\sigma}(\boldsymbol{u})\boldsymbol{n} = \mathbf{0} \text{ on } \partial S\times\mathbb{R}. \end{aligned}$$

The pulsation ω being given, approximations of these particular solutions are generally obtained by solving a quadratic eigenvalue problem resulting from a finite element discretization over the cross section of the waveguide (this is the so-called semi-analytical finite element (SAFE) method, see [12, 13] for a historic application to elastic layered orthotropic cylinders and plates). In the particular cases of a homogeneous plate (the Rayleigh–Lamb modes) or of a homogeneous circular rod (the Pochhammer–Chree modes), closed-form expressions of the modes are available and their determination reduces to a search for the zeros of a dispersion relation. It follows (see [14] for instance) from properties of the functional operators involved in the problem that the set of complex numbers β associated with the set of modes is both discrete and symmetric with respect to $\mathrm{Re}(\beta) = 0$ and $\mathrm{Im}(\beta) = 0$, a mode being said to be *propagative* if $\beta \in \mathbb{R}$, and *evanescent* if $\mathrm{Im}(\beta) \neq 0$.

The guided elastic modes also satisfy biorthogonality relations. To see this, let us denote respectively by $\boldsymbol{u}_S$ and u_d the transverse and axial components of the displacement field $\boldsymbol{u}$, and by $\boldsymbol{t}_S$ and t_d those of the normal stress $\boldsymbol{\sigma}(\boldsymbol{u})\boldsymbol{e}_d$. We then introduce the *hybrid* (since they include both displacement and stress tensor components) vector quantities

$$\boldsymbol{X} = \begin{pmatrix} \boldsymbol{t}_S \\ u_d \end{pmatrix} \text{ and } \boldsymbol{Y} = \begin{pmatrix} \boldsymbol{u}_S \\ -t_d \end{pmatrix},$$

as in [15, 16]. These new variables provide a particularly adequate approach to the characterization of modes, both from a theoretical (mathematical analysis) and practical (numerical computation, construction of transparent boundary conditions, etc...) perspective, since a triplet $(\beta, \mathbf{X}, \mathbf{Y})$ associated with a mode, that is, such that

$$\boldsymbol{X}(\boldsymbol{x}) = \mathbf{X}(\boldsymbol{x}_S)\, e^{\mathrm{i}\beta x_d} \text{ and } \boldsymbol{Y}(\boldsymbol{x}) = \mathbf{Y}(\boldsymbol{x}_S)\, e^{\mathrm{i}\beta x_d},$$

is solution to a linear eigenproblem (see again [14]). For this reason, we refer to such a triplet as an eigenelement in what follows.

Setting, for any $\mathbf{X}$ and $\mathbf{Y}$ in $L^2(S)^d$,

$$(\mathbf{X}|\mathbf{Y})_S = \int_S \sum_{i=1}^{d} \mathrm{X}_i \mathrm{Y}_i \,\mathrm{d}\boldsymbol{x}_S = \int_S \left(\mathbf{t}_S \cdot \mathbf{u}_S - \mathrm{u}_d \mathrm{t}_d\right) \mathrm{d}\boldsymbol{x}_S, \tag{4}$$

it can be seen that any pair of eigenelements $(\beta, \mathbf{X}, \mathbf{Y})$ and $(\widetilde{\beta}, \widetilde{\mathbf{X}}, \widetilde{\mathbf{Y}})$, $\widetilde{\beta} \neq \beta$, satisfies the following relation

$$(\widetilde{\beta}^2 - \beta^2)(\mathbf{X}|\widetilde{\mathbf{Y}})_S = 0.$$

In particular, one has $(\mathbf{X}|\widetilde{\mathbf{Y}})_S = 0$ as soon as $\widetilde{\beta} \neq -\beta$, which generalizes the relation for the Rayleigh–Lamb modes derived by Fraser [17]. This also means that an eigenelement $(\beta, \mathbf{X}, \mathbf{Y})$ is "orthogonal", in the sense of biorthogonal systems, to any other eigenelement $(\widetilde{\beta}, \widetilde{\mathbf{X}}, \widetilde{\mathbf{Y}})$, except if $\widetilde{\beta} = -\beta$, in which case the corresponding modes propagate in opposite directions. Defining the important notion of propagation direction requires to avoid the so-called *cut-off frequencies*. This is the object of the following hypothesis.

Assumption 1. *The pulsation ω is such that $(\mathbf{X}|\mathbf{Y})_S \neq 0$ for any eigenelement $(\beta, \mathbf{X}, \mathbf{Y})$.*

We conjecture that the set of values of the pulsation ω which do not meet assumption 1 is a countable subset of $\mathbb{R}_+$, but we do not know of any proof of this result. Now, assuming the wavenumber β is a smooth function of the pulsation ω, this hypothesis implies that the group velocity $\frac{\partial \omega}{\partial \beta}$ of a propagative mode does not vanish (see Lemma 4 and Remark 1 in [14]), which allows to define the propagation direction of the considered mode. We thus say that a propagative mode is *rightgoing* (resp. *leftgoing*) if its group velocity is positive (resp. negative). Accordingly, an evanescent mode is rightgoing (resp. leftgoing) if $\mathrm{Im}(\beta) > 0$ (resp. $\mathrm{Im}(\beta) < 0$). Note that, due to the chosen convention for the assumed time-dependance, a rightgoing (resp. leftgoing) mode propagates in the $x_d > 0$ (resp. $x_d < 0$) direction.

From now on, we denote by $(\beta_n, \mathbf{X}_n, \mathbf{Y}_n)$, $n \in \mathbb{N}$, an eigenelement corresponding to a rightgoing mode, counted with its multiplicity. It then results from simple symmetry arguments that $(-\beta_n, -\mathbf{X}_n, \mathbf{Y}_n)$, $n \in \mathbb{N}$, corresponds to a leftgoing mode. Since assumption 1 ensures that the quantity $(\mathbf{X}_n|\mathbf{Y}_n)_S$, $n \in \mathbb{N}$, is never zero, we can suppose, after a suitable normalization, that it holds

$$(\mathbf{X}_m|\mathbf{Y}_n)_S = \delta_{mn}, \ \forall m \in \mathbb{N}, \ \forall n \in \mathbb{N}. \tag{5}$$

Before we close this subsection, we formulate a conjecture about the localization of the wavenumbers β_n, $n \in \mathbb{N}$, in the complex plane.

Conjecture 1. *For any value of the pulsation ω and any real number δ in $[0, \frac{\pi}{2})$, there exist a positive integer N_δ and an ordering of the set $\{\beta_n\}_{n\in\mathbb{N}}$ such that one has*

$$n \geq N_\delta \Leftrightarrow |Im(\beta_n)| \geq \tan(\delta)\, |Re(\beta_n)|\,. \tag{6}$$

This conjecture implies in particular that there is a finite number $\mathcal{N}$, with $\mathcal{N} \leq N_\delta$, of propagative modes. This result is commonly admitted but, to the best of our knowledge, has never been rigorously proven in the general case. It holds true for Rayleigh–Lamb modes, as Merkulov *et al.* [18] derived the following asymptotic behavior

$$\beta_n\, h \sim \frac{\mathrm{i}n\pi}{2} \text{ as } n \to +\infty,$$

for rightgoing modes in a plate of height $2h$.

2.3 Modal expansion

As already mentioned, modal series expansions are extensively used in the sequel. The proper mathematical sense of these will not be discussed here, as it would raise several questions which are out of the scope of the present paper, even in the simple two-dimensional case of the Rayleigh–Lamb modes. We solely point out that, for any practical (that is, numerical) purpose, these expansions will always be truncated to a finite number of terms.

Consider a portion of the waveguide $S \times [x_d^-, x_d^+]$ and a solution $\boldsymbol{u}$ to the homogeneous equations

$$\begin{aligned} &-\rho\omega^2 \boldsymbol{u} - \mathrm{div}(\boldsymbol{\sigma}(\boldsymbol{u})) = \mathbf{0} \text{ in } S \times (x_d^-, x_d^+), \\ &\boldsymbol{\sigma}(\boldsymbol{u})\boldsymbol{n} = \mathbf{0} \text{ on } \partial S \times (x_d^-, x_d^+). \end{aligned}$$

By choosing a reference position z, $x_d^- \leq z \leq x_d^+$, the solution $\boldsymbol{u}$ can formally be expressed as a superposition of leftgoing and rightgoing modes in $S \times [x_d^-, x_d^+]$, that is

$$\boldsymbol{u}(\boldsymbol{x}) = \boldsymbol{u}(\boldsymbol{x}_S, x_d) = \sum_{n\in\mathbb{N}} \left(A_n^+(z)\, \mathbf{u}_n^+(\boldsymbol{x}_S)\, e^{\mathrm{i}\beta_n\,(x_d - z)} + A_n^-(z)\, \mathbf{u}_n^-(\boldsymbol{x}_S)\, e^{-\mathrm{i}\beta_n\,(x_d - z)} \right), \tag{7}$$

where

$$\mathbf{u}_n^+ = \begin{pmatrix} \mathbf{u}_{nS} \\ \mathrm{u}_{nd} \end{pmatrix} \text{ and } \mathbf{u}_n^- = \begin{pmatrix} \mathbf{u}_{nS} \\ -\mathrm{u}_{nd} \end{pmatrix}, \ \forall n \in \mathbb{N}.$$

In practice, the values of the modal coefficients $A_n^{\pm}(z)$, $n \in \mathbb{N}$, can be recovered from the knowledge of the displacement and axial stress fields on a given cross section, by considering the hybrid quantities $\boldsymbol{X}(\boldsymbol{u})$ and $\boldsymbol{Y}(\boldsymbol{u})$ and using the biorthogonality relation. Indeed, if the fields $\boldsymbol{X}(\boldsymbol{u})$ and $\boldsymbol{Y}(\boldsymbol{u})$ are known for a given $x_d \in (x_d^-, x_d^+)$ and any $\boldsymbol{x}_S$ in S, one has on the one hand

$$\boldsymbol{X}(\boldsymbol{u})(\boldsymbol{x}_S, x_d) = \sum_{n\in\mathbb{N}} \left(A_n^+(z)\, e^{\mathrm{i}\beta_n\,(x_d - z)} - A_n^-(z)\, e^{-\mathrm{i}\beta_n\,(x_d-z)} \right) \mathbf{X}_n(\boldsymbol{x}_S),$$

and

$$\boldsymbol{Y}(\boldsymbol{u}_S, x_d)(\boldsymbol{x}) = \sum_{n\in\mathbb{N}} \left(A_n^+(z)\, e^{\mathrm{i}\beta_n\,(x_d - z)} + A_n^-(z)\, e^{-\mathrm{i}\beta_n\,(x_d-z)} \right) \mathbf{Y}_n(\boldsymbol{x}_S)$$

on the other. It then results from (5) that

$$\begin{aligned}
(\boldsymbol{X}(\boldsymbol{u})(\cdot, x_d)|\mathbf{Y}_n)_S &= A_n^+(z)\, e^{\mathrm{i}\beta_n\,(x_d - z)} - A_n^-(z)\, e^{-\mathrm{i}\beta_n\,(x_d-z)},\\
(\mathbf{X}_n|\boldsymbol{Y}(\boldsymbol{u})(\cdot, x_d))_S &= A_n^+(z)\, e^{\mathrm{i}\beta_n\,(x_d - z)} + A_n^-(z)\, e^{-\mathrm{i}\beta_n\,(x_d-z)},
\end{aligned}$$

the modal coefficients being easily obtained by solving a two by two linear system. When the data set is given on the cross-section corresponding to $x_d = z$, one is led to the following formulas for the coefficients

$$A_n^+(z) = \frac{1}{2}\left((\boldsymbol{X}(\boldsymbol{u})(\cdot, z)|\mathbf{Y}_n)_S + (\mathbf{X}_n|\boldsymbol{Y}(\boldsymbol{u})(\cdot, z))_S \right),\ n \in \mathbb{N}, \tag{8}$$

$$A_n^-(z) = \frac{1}{2}\left((\boldsymbol{X}(\boldsymbol{u})(\cdot, z)|\mathbf{Y}_n)_S - (\mathbf{X}_n|\boldsymbol{Y}(\boldsymbol{u})(\cdot, z))_S \right),\ n \in \mathbb{N}. \tag{9}$$

Note that these coefficients depend linearly on the displacement field $\boldsymbol{u}$, and we thus use the notation $A_n^{\pm}(z;\boldsymbol{u})$, $n \in \mathbb{N}$, whenever this dependence ought to be precised in the forthcoming developments.

2.4 The diffraction-radiation problem

Let us finally define a problem set in the semi-infinite waveguide Ω introduced in subsection 2.1. Without loss of generality, we may consider an incident field $\boldsymbol{u}_{\mathrm{inc}}$ in the form of a leftgoing propagative mode

$$\boldsymbol{u}_{\mathrm{inc}}(\boldsymbol{x}) = \mathbf{u}_\ell^-(\boldsymbol{x}_S)\, e^{-\mathrm{i}\beta_\ell\, x_d},$$

with ℓ a fixed natural number, and a source term $\boldsymbol{f}$, accounting for a volumic density of body forces, in $L^2(\Omega)^d$ with compact support in the region Ω_0. We look for the displacement field $\boldsymbol{u}$ in $H^1_{\mathrm{loc}}(\Omega)^d$ which satisfies, in an appropriate sense, the following system

$$\begin{aligned}
&-\rho\omega^2\boldsymbol{u} - \mathrm{div}(\boldsymbol{\sigma}(\boldsymbol{u})) = \boldsymbol{f} \text{ in } \Omega,\\
&\boldsymbol{\sigma}(\boldsymbol{u})\boldsymbol{n} = \mathbf{0} \text{ on } \partial\Omega,\\
&\boldsymbol{u}_{\mathrm{sca}} = \boldsymbol{u} - \boldsymbol{u}_{\mathrm{inc}} \text{ is a superposition of rightgoing modes in } \Omega_+,
\end{aligned} \tag{10}$$

which can be viewed as a diffraction (when the source term $\boldsymbol{f}$ vanishes) and/or radiation (when there is no incident field) problem. The last condition in (10) expresses that the solution is *outgoing*. It also means that the modal coefficients A_n^-, $n \in \mathbb{N}$, vanish in the expansion (7) of the field $\boldsymbol{u}_{\mathrm{sca}}$, so that

$$\boldsymbol{u}_{\mathrm{sca}}(\boldsymbol{x}_S, x_d) = \sum_{n\in\mathbb{N}} A_n^+(0;\boldsymbol{u}_{\mathrm{sca}})\, \mathbf{u}_n^+(\boldsymbol{x}_S)\, e^{\mathrm{i}\beta_n\, x_d},\ \boldsymbol{x}_S \in S,\ x_d \in [0, +\infty).$$

Note that problem (10) is of Fredholm type and may be ill-posed. Indeed, there exist values of the pulsation ω, forming at most a countable set, for which uniqueness of the solution is lacking. In this very case, observe that, by linearity, there exists a nontrivial field $\boldsymbol{w}$ satisfying

$$\begin{aligned}
&-\rho\omega^2\boldsymbol{w} - \mathrm{div}(\boldsymbol{\sigma}(\boldsymbol{w})) = \mathbf{0} \text{ in } \Omega,\\
&\boldsymbol{\sigma}(\boldsymbol{w})\boldsymbol{n} = \mathbf{0} \text{ on } \partial\Omega,
\end{aligned}$$

which is outgoing, hence admitting a representation of the form

$$\boldsymbol{w}(\boldsymbol{x}_S, x_d) = \sum_{n\in\mathbb{N}} A_n^+(0;\boldsymbol{w})\, \mathbf{u}_n^+(\boldsymbol{x}_S)\, e^{\mathrm{i}\beta_n\, x_d},\ \boldsymbol{x}_S \in S,\ x_d \in [0, +\infty).$$

As non-propagative modes do not carry energy (see for instance [16, section 4]), the energy conservation relation then yields

$$\sum_{n=1}^{\mathcal{N}} \left|A_n^+(0;\boldsymbol{w})\right|^2 = 0,$$

where $\mathcal{N}$ denotes the number of propagative modes, hence $A_n^+(0;\boldsymbol{w}) = 0$, $\forall n \in \{1,\dots,\mathcal{N}\}$. In other words, any solution of the homogeneous problem can be decomposed on the evanescent modes for $x_d > 0$. Such a field being exponentially decaying at infinity, this solution is called a *trapped* mode (see [19] for instance). By making the following postulate, problem (10) is well-posed.

Assumption 2. *The configuration of problem* (10) *is such that there are no trapped modes.*

When devising a numerical method to approximate the solution to problem (10), the main difficulty is to derive a formulation of the problem which is both set in a bounded domain and able to accurately handle the propagative nature of the scattered field at infinity. For classical scattering problems, one of the simplest ways to accomplish this is to employ perfectly matched layers, as explained in the next section. However, this technique is sometimes discarded in elastic waveguides, because it fails when backward propagating modes are present (see [8] for instance). Alternative solutions, which use the modal representation, have been developed [20, 14, 21], but they may require specific implementation efforts. In section 4, we propose a strategy which combines the simplicity of the PML methods with the accuracy of the modal ones.

3 Perfectly matched layers

We now describe and discuss the application of the PML technique to the problem introduced in the preceding section. References pertaining to PML for time-harmonic elastic wave propagation problems are, for instance, [22, 23, 8, 24]. Here, only the most straighforward kind of PML, that is, with constant coefficients, is considered, but the whole reasoning still applies if these coefficients are complex-valued functions of the space variables satisfying the conditions stated below. One might note in passing that optimizing the choice of the absorbing function for a bounded layer, as done in [25] for instance, cannot cure the problem caused by the presence of backward modes, as can be seen from a straightforward extension of the analysis in subsection 3.2 (see remark 1).

3.1 General presentation

The PML method aims at constructing an artificial medium to be placed adjacent to the region of interest and designed in such a way that the waves entering it are not reflected at its interface with the "physical" medium and decay exponentially into it. To achieve such features, a complex (in the sense of imaginary numbers) coordinate stretching is used, as was observed in [26, 27], to analytically continue the solution to the problem along a given contour in the complex plane.

Let us thus introduce a complex number α, whose precise value will be discussed later, and consider the analytically stretched *scattered* displacement field, denoted by $\boldsymbol{u}_\alpha$, associated with the solution to problem (10) in the unbounded domain Ω_+,

$$\boldsymbol{u}_\alpha(\boldsymbol{x}_S, x_d) = \boldsymbol{u}_{\text{sca}}\left(\boldsymbol{x}_S, \frac{x_d}{\alpha}\right) = \sum_{n\in\mathbb{N}} A_n^+(0;\boldsymbol{u}_{\text{sca}})\,\mathbf{u}_n^+(\boldsymbol{x}_S)\,e^{\mathrm{i}\beta_n \frac{x_d}{\alpha}},\ \boldsymbol{x}_S \in S, x_d \in [0,+\infty).$$

One immediately remarks that the analytic continuation is expressed as a coordinate transformation in the (infinite) layer Ω_+, which may thus be seen as made of some homogeneous artificial anisotropic medium. As a consequence, the equations defining problem (10) are replaced by the following system,

$$\begin{aligned}
&-\rho\omega^2\boldsymbol{u} - \operatorname{div}(\boldsymbol{\sigma}(\boldsymbol{u})) = \boldsymbol{f} \text{ in } \Omega_0,\\
&-\rho\omega^2\boldsymbol{u}_\alpha - \operatorname{div}_\alpha(\boldsymbol{\sigma}_\alpha(\boldsymbol{u}_\alpha)) = \mathbf{0} \text{ in } \Omega_+,\\
&\boldsymbol{\sigma}(\boldsymbol{u})\boldsymbol{n} = \mathbf{0} \text{ on } \partial\Omega_0 \cap \partial\Omega,\\
&\boldsymbol{\sigma}_\alpha(\boldsymbol{u}_\alpha)\boldsymbol{n} = \mathbf{0} \text{ on } \partial\Omega_+ \cap \partial\Omega,
\end{aligned} \tag{11}$$

supplemented by the transmission conditions on the interface $\Sigma_+ = \partial\Omega_0 \cap \partial\Omega_+$

$$\begin{aligned}
&\boldsymbol{u} - \boldsymbol{u}_{\text{inc}} = \boldsymbol{u}_\alpha \text{ on } \Sigma_+,\\
&\boldsymbol{\sigma}(\boldsymbol{u} - \boldsymbol{u}_{\text{inc}})\boldsymbol{e}_d = \boldsymbol{\sigma}_\alpha(\boldsymbol{u}_\alpha)\boldsymbol{e}_d \text{ on } \Sigma_+,
\end{aligned} \tag{12}$$

whose unknowns are the total displacement field $\boldsymbol{u}$ in the bounded domain Ω_0, and the field $\boldsymbol{u}_\alpha$ in Ω_+. The equations in the layer have been modified to account for the coordinate transformation by making the substitution

$$\frac{\partial}{\partial x_d} \to \alpha \frac{\partial}{\partial x_d}$$

in the expressions of the differential operators, which are therefore indexed by α. For instance, one has

$$\boldsymbol{\sigma}_\alpha(\boldsymbol{v}) = \lambda \, \mathrm{div}_\alpha(\boldsymbol{v}) \, \mathbf{I} + \mu \left(\boldsymbol{\nabla}_\alpha \boldsymbol{v} + (\boldsymbol{\nabla}_\alpha \boldsymbol{v})^T \right),$$

with

$$\mathrm{div}_\alpha(\boldsymbol{v}) = \mathrm{div}_S(\boldsymbol{v}_S) + \alpha \frac{\partial v_d}{\partial x_d} \text{ and } \boldsymbol{\nabla}_\alpha \boldsymbol{v} = \begin{pmatrix} \boldsymbol{\nabla}_S \boldsymbol{v}_S & \alpha \dfrac{\partial \boldsymbol{v}_S}{\partial x_d} \\ \boldsymbol{\nabla}_S v_d & \alpha \dfrac{\partial v_d}{\partial x_d} \end{pmatrix}.$$

The scattered field being analytically continued in Ω_+, the solution to the above system of equations remains, when compared to the solution to (10), unchanged in the domain Ω_0, and no reflection occurs at the interface between Ω_0 and Ω_+: the layer is said to be *perfectly matched*.

Next, for the layer to be truncated at finite distance, the complex medium also has to act as an absorbing material, so that the quantity $\boldsymbol{u}_\alpha(\boldsymbol{x})$ decays exponentially in the layer as x_d increases. In other words, any stretched rightgoing mode of the form

$$\mathbf{u}_n(\boldsymbol{x}_S) \, e^{\mathrm{i} \frac{\beta_n}{\alpha} x_d}, \ n \in \mathbb{N},$$

has to decay exponentially in the domain Ω_+ as x_d increases ; obviously, this holds if

$$\mathrm{Im}\left(\frac{\beta_n}{\alpha} \right) > 0, \ \forall n \in \mathbb{N}. \tag{13}$$

Let us examine which values of the coefficient α should be used in practice to achieve the above inequality. On the one hand, a propagative mode being such that its associated wavenumber is real, its decay in the layer depends crucially on the sign of its wavenumber. In the most common case, a rightgoing propagative mode corresponds to a wavenumber β_n which is positive (which means that the mode has a positive phase velocity $\frac{\omega}{\beta_n}$). Hence, choosing the complex coefficient α with a negative imaginary part ensures that the stretched mode is evanescent in the layer.

We may therefore set from now on $\alpha = |\alpha| \ e^{-\mathrm{i}\theta}$, with $0 < \theta < \frac{\pi}{2}$. This choice is consistent with the one usually made in the literature, stemming from time-dependent applications, for which the coefficient α is a function of the form

$$\alpha = \frac{-\mathrm{i}\omega}{-\mathrm{i}\omega + \sigma},$$

where σ is an increasing positive, possibly constant, function of the variable x_d. Unfortunately, a peculiar feature of elastic waveguides is the existence, in some frequency bands depending on the material, of some backward propagating modes, for which the group velocity and the phase velocity have opposite signs (see Figure 2 for an example). As a consequence, any value of the coefficient α that makes the forward propagative modes exponentially decreasing in the layer will also make the backward modes exponentially increasing. This very difficulty[2] is the motivation behind the present work.

On the other hand, the evanescent rightgoing modes have to remain exponentially decaying after being stretched. Since their associated wavenumbers are such that $0 < \arg(\beta_n) < \pi$, the condition (13) can be equivalently written

$$\mathrm{Im}(\beta_n) + \tan(\theta) \, \mathrm{Re}(\beta_n) > 0. \tag{14}$$

Using the conjecture materialized in (6), we clearly see that the last condition is not satisfied by at most a finite number, which we denote by $\mathcal{N}(\theta)$, of rightgoing modes. These are the backward propagating modes (such that $\mathrm{Im}(\beta_n) = 0$ and $\mathrm{Re}(\beta_n) < 0$) and, possibly, some evanescent modes. One easily checks that the larger the angle θ, the smaller the integer $\mathcal{N}(\theta)$, but, in any case, this number is greater than or equal to the number of backward propagating modes.

[2] We insist on the fact that it is the coexistence of forward and backward propagating rightgoing modes which does pose a problem. Indeed, in the case where the real wavenumbers all have the "wrong" sign (like in left-handed materials for instance), the PML technique can be successfully applied by means of a slight modification (see [28, 29]).

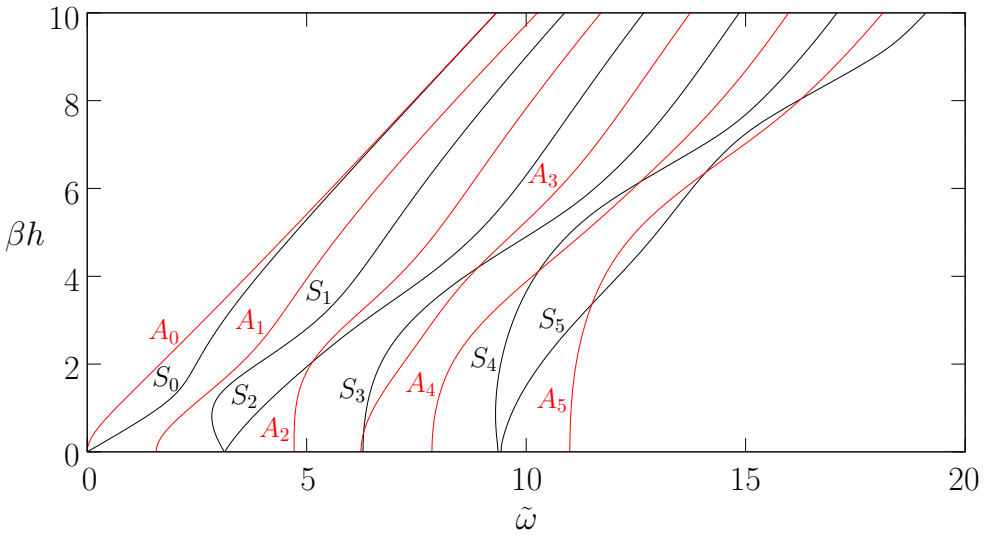

Figure 2: Dispersion curves, derived from the dispersion relation $\frac{\omega^4}{{c_s}^4} = 4\beta^2{\alpha_s}^2\left(1 - \frac{\alpha_p \tan(\alpha_p h+\kappa)}{\alpha_s \tan(\alpha_s h+\kappa)}\right)$, with $\alpha_p = \sqrt{\beta^2 - \frac{\omega^2}{{c_p}^2}}$ and $\alpha_s = \sqrt{\beta^2 - \frac{\omega^2}{{c_s}^2}}$ and where $c_p = \sqrt{\frac{\lambda+2\mu}{\rho}}$ is the longitudinal (pressure) wave velocity and $c_s = \sqrt{\frac{\mu}{\rho}}$ is the shear wave velocity, for symmetric ($\kappa = 0$, in black) and antisymmetric ($\kappa = \frac{\pi}{2}$, in red) propagative Rayleigh–Lamb modes in a plate of thickness $2h$ made of a material with Poisson's ratio ν equal to 0.33 (aluminium for instance), the dimensionless variable $\tilde{\omega}$ being equal to $\frac{\omega h}{c_s}$. Inspection of the second and fifth curves associated with the symmetric modes reveals that backward propagating modes exist at low frequencies.

3.2 Truncation of the layer

When the number $\mathcal{N}(\theta)$ is zero (which means in particular that no backward propagating mode exists), the diffracted field is exponentially decaying in the layer. It may therefore be considered negligible for a sufficiently large x_d, which allows to truncate the layer at some finite distance $x_d = L > 0$. Various conditions can be imposed at the artificial boundary $\Sigma_+^L = S \times \{L\}$, such as the vanishing of the displacement $\boldsymbol{u}_\alpha$ (that is, a homogeneous Dirichlet boundary condition) or that of the axial stress $\boldsymbol{\sigma}_\alpha(\boldsymbol{u}_\alpha)\boldsymbol{e}_d$ (a homogeneous Neumann-type boundary condition). Alternatively, one can also opt for a homogeneous boundary condition on a mixed quantity such as $\boldsymbol{X}_\alpha(\boldsymbol{u}_\alpha)$ or $\boldsymbol{Y}_\alpha(\boldsymbol{u}_\alpha)$, the advantage, both from a theoretical and numerical point of view, of this latter choice being that it does not produce mode conversion by reflection on the boundary. In what follows, we set $\boldsymbol{Y}_\alpha(\boldsymbol{u}_\alpha) = \boldsymbol{0}$ on Σ_+^L, which means that we impose the vanishing of both the transverse stretched displacement, $\boldsymbol{u}_{\alpha S}$, and the axial component of the stretched axial stress, $t_{\alpha d}(\boldsymbol{u}_\alpha)$.

The problem to be solved, set in the bounded domain $\Omega^L = \Omega_0 \cup \Omega_+^L$, where $\Omega_+^L = S \times (0, L)$ is the perfectly matched layer, then consists of the following set of equations

$$
\begin{aligned}
&-\rho\omega^2\boldsymbol{u}^L - \operatorname{div}(\boldsymbol{\sigma}(\boldsymbol{u}^L)) = \boldsymbol{f} \text{ in } \Omega_0,\\
&-\rho\omega^2\boldsymbol{u}_\alpha^L - \operatorname{div}_\alpha(\boldsymbol{\sigma}_\alpha(\boldsymbol{u}_\alpha^L)) = \boldsymbol{0} \text{ in } \Omega_+^L,\\
&\boldsymbol{\sigma}(\boldsymbol{u}^L)\boldsymbol{n} = \boldsymbol{0} \text{ on } \partial\Omega \cap \partial\Omega_0,\\
&\boldsymbol{\sigma}_\alpha(\boldsymbol{u}_\alpha^L)\boldsymbol{n} = \boldsymbol{0} \text{ on } \partial\Omega \cap \partial\Omega_+^L,\\
&\boldsymbol{u}^L - \boldsymbol{u}_{\text{inc}} = \boldsymbol{u}_\alpha^L \text{ on } \Sigma_+,\\
&\boldsymbol{\sigma}(\boldsymbol{u}^L - \boldsymbol{u}_{\text{inc}})\boldsymbol{e}_d = \boldsymbol{\sigma}_\alpha(\boldsymbol{u}_\alpha^L)\boldsymbol{e}_d \text{ on } \Sigma_+,\\
&(\boldsymbol{u}_\alpha^L)_S = \boldsymbol{0},\ t_{\alpha d}(\boldsymbol{u}_\alpha^L) = 0 \text{ on } \Sigma_+^L,
\end{aligned}
\tag{15}
$$

the unknown in Ω_0 being denoted by $\boldsymbol{u}^L$, the one in Ω_+^L is by $\boldsymbol{u}_\alpha^L$.

The solution to this problem is one of the main ingredients of our method and we formulate the following hypothesis, which is discussed in section 7.

Assumption 3. *Problem* (15) *is well-posed.*

Depending on the absence or the presence of backward propagating modes, the solution $\boldsymbol{u}^L$ may or may not be a valid approximation to the exact solution $\boldsymbol{u}$ to (10) in Ω_0, the error being due to the truncation and the non-exact

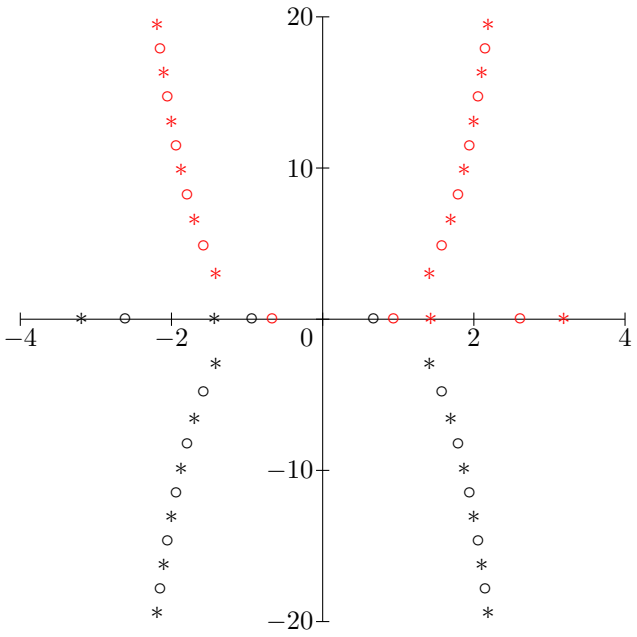

Figure 3: Positions in the complex plane of the first wavenumbers $\pm\beta_n$ respectively associated with rightgoing (in red) and leftgoing (in black) Rayleigh–Lamb modes (the symbols $\circ$ (resp. $*$) refer to symmetric (resp. antisymmetric) modes) in an aluminium ($\rho = 2700$ kg m^{-1}, $E = 69$ GPa, and $\nu = 0.33$) plate of thickness 2 m at low frequency ($\omega = 8833.7825$ rad s^{-1}). Two wavenumbers are associated to backward propagating symmetric modes.

boundary condition imposed at the back end of the layer. To measure it, we proceed as in subsection 2.3, starting by expressing the field $\boldsymbol{u}_\alpha^L$ in the layer as a superposition of stretched modes,

$$\boldsymbol{u}_\alpha^L(\boldsymbol{x}) = \sum_{n\in\mathbb{N}} \left(A_n^+(0;\boldsymbol{u}_\alpha^L)\,\mathbf{u}_n^+(\boldsymbol{x}_S)\,e^{\mathrm{i}\frac{\beta_n}{\alpha}x_d} + A_n^-(0;\boldsymbol{u}_\alpha^L)\,\mathbf{u}_n^-(\boldsymbol{x}_S)\,e^{-\mathrm{i}\frac{\beta_n}{\alpha}x_d} \right),\ \forall \boldsymbol{x}\in\Omega_+^L,$$

the boundary condition at the end of the layer yielding the following relation between the rightgoing and leftgoing stretched modes,

$$A_n^+(0;\boldsymbol{u}_\alpha^L)\,e^{\mathrm{i}\frac{\beta_n}{\alpha}L} + A_n^-(0;\boldsymbol{u}_\alpha^L)\,e^{-\mathrm{i}\frac{\beta_n}{\alpha}L} = 0,\ \forall n\in\mathbb{N}. \tag{16}$$

Introducing the reflection coefficient $R_n(\alpha, L)$, $n\in\mathbb{N}$, defined as

$$A_n^-(0;\boldsymbol{u}_\alpha^L) = R_n(\alpha,L)\,A_n^+(0;\boldsymbol{u}_\alpha^L),$$

we obtain from (16) the following equality

$$R_n(\alpha,L) = -e^{2\mathrm{i}\frac{\beta_n}{\alpha}L}, \tag{17}$$

which constitutes the basis for the estimation of the error of the method.

We therefore observe that the error manifests itself in the existence of reflected modes in the approximate solution[3]. The method will be deemed accurate if these reflections are small or, more properly, if the reflection coefficients $R_n(\alpha, L)$, $\forall n\in\mathbb{N}$, are small, the values of the parameters α and L being fixed. As discussed in the previous subsection, this depends critically on the behavior, either attenuated or amplified, of the stretched modes in the PML. Using the classification given in subsection 3.1, suppose that the $\mathcal{N}(\theta)$ modes which are amplified correspond to the indices $n = 0, 1, \ldots, \mathcal{N}(\theta)-1$. For these, the reflection coefficient $R_n(\alpha, L)$ tends to infinity with L (or as $|\alpha|$ tends to zero), since the corresponding imaginary part $\mathrm{Im}\left(\frac{\beta_n}{\alpha}\right)$ is negative. Reflections on the n^{th} mode are then not negligible and can even overwhelm the outgoing modes in the approximate solution, rendering the method completely useless in practice.

[3]Let us recall that, for the exact solution, one has $A_n^-(0;\boldsymbol{u}) = 0$, $\forall n\in\mathbb{N}$.

On the other hand, for $n \geq \mathcal{N}(\theta)$, the value of $R_n(\alpha, L)$ can be made arbitrarily small by taking L large enough (and/or $|\alpha|$ small enough). Observe nevertheless that very small, but non-zero, values of β_n will be detrimental to the performance of the method, as they produce reflections which may be non negligible unless the layer is quite thick (and/or $|\alpha|$ is quite small), thus inducing an increase of the computational cost in practice.

As we now see, from a practical point of view, the modes responsible for the error of the method are not only the backward ones, but also the long ones (that is, those associated with an almost vanishing wavenumber β_n). A prescribed tolerance ε being given and the parameters α and L being fixed, we introduce the number $\mathcal{N}_\varepsilon(\alpha, L)$ such that, for all n in $\mathbb{N}$,

$$n \geq \mathcal{N}_\varepsilon(\alpha, L) \Longleftrightarrow |R_n(\alpha, L)| \leq \varepsilon. \tag{18}$$

By definition of the reflection coefficients, this is equivalent to

$$n \geq \mathcal{N}_\varepsilon(\alpha, L) \Longleftrightarrow \mathrm{Im}\left(\frac{\beta_n}{\alpha}\right) \geq \frac{|\ln(\varepsilon)|}{2\,L},$$

which shows that $\mathcal{N}_\varepsilon(\alpha, L) \geq \mathcal{N}(\theta)$. It is clear that the solution $\boldsymbol{u}^L$ cannot be an accurate approximation, that is, with an error of order of magnitude ε, of the exact solution $\boldsymbol{u}$ whenever $\mathcal{N}_\varepsilon(\alpha, L)$ is non-zero. We present in the next section a strategy to correct this misbehavior of the PML technique in such cases.

Remark 1. *Let us mention that the previous analysis can be easily extended to a PML with a varying (and non vanishing) coefficient α, function of the variable x_d. Following the computation in [30, section 4], we see that* (17) *becomes*

$$R_n(\alpha, L) = -e^{2\mathrm{i}\beta_n \int_0^L \frac{\mathrm{d}s}{\alpha(s)}},$$

so that (18) *is then equivalent to*

$$n \geq \mathcal{N}_\varepsilon(\alpha, L) \Longleftrightarrow Im\left(\beta_n \left\langle \frac{1}{\alpha} \right\rangle\right) \geq \frac{|\ln(\varepsilon)|}{2\,L},$$

where $\left\langle \frac{1}{\alpha} \right\rangle$ stands for the mean of $\frac{1}{\alpha}$ over $(0, L)$,

$$\left\langle \frac{1}{\alpha} \right\rangle = \frac{1}{L} \int_0^L \frac{\mathrm{d}s}{\alpha(s)}.$$

4 Strategy for treating backward and long waves

We suppose from now on that the number $\mathcal{N}_\varepsilon(\alpha, L)$, denoted briefly by $\mathcal{N}_\varepsilon$ in the remainder of the paper, is not equal to zero.

As explained in the previous section, the solution $(\boldsymbol{u}^L, \boldsymbol{u}_\alpha^L)$ of problem (15) differs *a priori* largely from the restriction to Ω^L of the solution $(\boldsymbol{u}, \boldsymbol{u}_\alpha)$ to problem (11), due to spurious reflections on the $\mathcal{N}_\varepsilon$ "first" guided modes of the waveguide caused by the truncation of the PML. In order to provide a cure, let us examine problem (15), keeping problem (11) in perspective.

We first remark that part of the system of equations defining the problem with truncated layers is exactly satisfied by the restriction of the solution $(\boldsymbol{u}, \boldsymbol{u}_\alpha)$ to Ω^L. These are the equations set in the domains Ω_0 and Ω_+^L, the conditions on the boundary of the waveguide, as well as the matching conditions on the interface between Ω_0 and Ω_+^L. These relations, which correspond to the first six equations in (15), are formally summarized in what follows by the equality

$$\mathcal{L}(\boldsymbol{u}^L, \boldsymbol{u}_\alpha^L) = (\boldsymbol{f}, \boldsymbol{u}_{\mathrm{inc}}),$$

where $\mathcal{L}$ is a linear operator and the fields $\boldsymbol{f}$ and $\boldsymbol{u}_{\mathrm{inc}}$ are the data of the problem. The only remaining equation in (15) not satisfied by $(\boldsymbol{u}, \boldsymbol{u}_\alpha)$ is the boundary condition imposed at the end of the layer. This is due to the spurious reflections on the $\mathcal{N}_\varepsilon$ first modes of the guide, characterized by

$$A_n^-(0; \boldsymbol{u}_\alpha^L) = R_n(\alpha, L)\, A_n^+(0; \boldsymbol{u}_\alpha^L),\ n = 0, \ldots, \mathcal{N}_{\varepsilon-1},$$

the reflection coefficient $R_n(\alpha, L)$ being given by (17).

Building on these observations, our aim is to propose a procedure for constructing a new approximation of the solution, in the form of a pair $(\widetilde{\boldsymbol{u}}^L, \widetilde{\boldsymbol{u}}_\alpha^L)$, related to the previous one, which satisfies

$$\mathcal{L}(\widetilde{\boldsymbol{u}}^L, \widetilde{\boldsymbol{u}}_\alpha^L) = (\boldsymbol{f}, \boldsymbol{u}_{\mathrm{inc}}), \tag{19}$$

and also is *quasi-outgoing*, in the sense that

$$\widetilde{\boldsymbol{u}}_\alpha^L(\boldsymbol{x}) = \sum_{n\in\mathbb{N}} \left(A_n^+(0;\widetilde{\boldsymbol{u}}_\alpha^L)\,\mathbf{u}_n^+(\boldsymbol{x}_S)\,e^{\mathrm{i}\frac{\beta_n}{\alpha}x_d} + A_n^-(0;\widetilde{\boldsymbol{u}}_\alpha^L)\,\mathbf{u}_n^-(\boldsymbol{x}_S)\,e^{-\mathrm{i}\frac{\beta_n}{\alpha}x_d}\right),\ \forall \boldsymbol{x}\in\Omega_+^L,$$

with

$$A_n^-(0;\widetilde{\boldsymbol{u}}_\alpha^L) = 0 \text{ if } n = 0,\dots,\mathcal{N}_\varepsilon - 1, \tag{20}$$

and

$$A_n^-(0;\widetilde{\boldsymbol{u}}_\alpha^L) = R_n(\alpha,L)\,A_n^+(0;\widetilde{\boldsymbol{u}}_\alpha^L) \text{ if } n \geq \mathcal{N}_\varepsilon. \tag{21}$$

In other words, we want the approximate solution to be completely free of reflections on the first $\mathcal{N}_\varepsilon$ guided modes, the ones on the other modes being negligible due to a sufficiently effective damping in the PML. In the physical domain Ω_0, the field $\widetilde{\boldsymbol{u}}^L$ will thus represent an accurate approximation of the exact solution $\boldsymbol{u}$, with an error magnitude of the order of the prescribed tolerance.

To obtain such a feature, let us consider the auxiliary fields $(\boldsymbol{w}^{(k)}, \boldsymbol{w}_\alpha^{(k)})$, $k = 0,\dots,\mathcal{N}_\varepsilon - 1$, respectively defined as the solutions to the following series of problems

$$\begin{aligned}
&-\rho\omega^2\boldsymbol{w}^{(k)} - \mathrm{div}(\boldsymbol{\sigma}(\boldsymbol{w}^{(k)})) = \mathbf{0} \text{ in } \Omega_0,\\
&-\rho\omega^2\boldsymbol{w}_\alpha^{(k)} - \mathrm{div}_\alpha(\boldsymbol{\sigma}_\alpha(\boldsymbol{w}_\alpha^{(k)})) = \mathbf{0} \text{ in } \Omega_+^L,\\
&\boldsymbol{\sigma}(\boldsymbol{w}^{(k)})\boldsymbol{n} = \mathbf{0} \text{ on } \partial\Omega\cap\partial\Omega_0,\\
&\boldsymbol{\sigma}_\alpha(\boldsymbol{w}_\alpha^{(k)})\boldsymbol{n} = \mathbf{0} \text{ on } \partial\Omega\cap\partial\Omega_+^L,\\
&\boldsymbol{w}^{(k)} = \boldsymbol{w}_\alpha^{(k)} - \boldsymbol{u}_{k,\alpha},\ \boldsymbol{\sigma}_\alpha(\boldsymbol{w}^{(k)})\boldsymbol{n} = \boldsymbol{\sigma}_\alpha(\boldsymbol{w}_\alpha^{(k)} - \boldsymbol{u}_{k,\alpha})\boldsymbol{n} \text{ on } \Sigma_+,\\
&(\boldsymbol{w}_\alpha^{(k)})_S = \mathbf{0},\ t_{\alpha d}(\boldsymbol{w}_\alpha^{(k)}) = 0 \text{ on } \Sigma_+^L,
\end{aligned}$$

where

$$\boldsymbol{u}_{k,\alpha}(\boldsymbol{x}) = \mathbf{u}_k^+(\boldsymbol{x}_S)\,e^{\mathrm{i}\frac{\beta_k}{\alpha}x_d},\ \forall\boldsymbol{x}\in\Omega_+^L,\ k = 0,\dots,\mathcal{N}_\varepsilon - 1. \tag{22}$$

It is easy to see that these auxiliary fields are linearly independent and such that

$$\mathcal{L}(\boldsymbol{w}^{(k)}, \boldsymbol{w}_\alpha^{(k)} - \boldsymbol{u}_{k,\alpha}) = (\mathbf{0},\mathbf{0}),$$

and

$$\boldsymbol{w}_\alpha^{(k)}(\boldsymbol{x}) = \sum_{n\in\mathbb{N}} \left(A_n^+(0;\boldsymbol{w}_\alpha^{(k)})\,\mathbf{u}_n^+(\boldsymbol{x}_S)\,e^{\mathrm{i}\frac{\beta_n}{\alpha}x_d} + A_n^-(0;\boldsymbol{w}_\alpha^{(k)})\,\mathbf{u}_n^-(\boldsymbol{x}_S)\,e^{-\mathrm{i}\frac{\beta_n}{\alpha}x_d}\right),\ \forall\boldsymbol{x}\in\Omega_+^L,$$

with

$$A_n^-(0;\boldsymbol{w}_\alpha^{(k)}) = R_n(\alpha,L)A_n^+(0;\boldsymbol{w}_\alpha^{(k)}) \text{ if } n \geq \mathcal{N}_\varepsilon.$$

The next result shows that $(\widetilde{\boldsymbol{u}}^L, \widetilde{\boldsymbol{u}}_\alpha^L)$ can be expressed as a linear combination involving the solution $(\boldsymbol{u}^L, \boldsymbol{u}_\alpha^L)$ and the set of auxiliary fields $(\boldsymbol{w}^{(k)}, \boldsymbol{w}_\alpha^{(k)})$, $k = 0,\dots,\mathcal{N}_\varepsilon - 1$.

Lemma 1. *Suppose that the problem defined by* (19), (20) *and* (21) *is well-posed. Then, there exist* $\mathcal{N}_\varepsilon$ *coefficients* $\mu^{(k)}$, $k = 0,\dots,\mathcal{N}_\varepsilon - 1$, *such that the field* $(\widetilde{\boldsymbol{u}}^L, \widetilde{\boldsymbol{u}}_\alpha^L)$ *given by*

$$\widetilde{\boldsymbol{u}}^L = \boldsymbol{u}^L + \sum_{k=0}^{\mathcal{N}_\varepsilon-1} \mu^{(k)}\,\boldsymbol{w}^{(k)},\ \widetilde{\boldsymbol{u}}_\alpha^L = \boldsymbol{u}_\alpha^L + \sum_{k=0}^{\mathcal{N}_\varepsilon-1} \mu^{(k)}\,\left(\boldsymbol{w}_\alpha^{(k)} - \boldsymbol{u}_{k,\alpha}\right), \tag{23}$$

satisfies (19), (20) *and* (21), *the coefficients* $\mu^{(k)}$ *being the unique solution of the linear system*

$$A_n^-(0;\boldsymbol{u}_\alpha^L) + \sum_{k=0}^{\mathcal{N}_\varepsilon-1} \mu^{(k)}\,A_n^-(0;\boldsymbol{w}_\alpha^{(k)}) = 0,\ n = 0,\dots,\mathcal{N}_\varepsilon - 1. \tag{24}$$

Proof. By linearity, it is clear that the equations (19) and (21) are satisfied for any value of the coefficients $\mu^{(k)}$. Since $A_n^-(0;\boldsymbol{u}_{k,\alpha}) = 0$, $k = 0,\dots,\mathcal{N}_\varepsilon - 1$, it is a simple matter, using (23), to see that the equations (20) are equivalent to the linear system (24).

It remains to prove that this linear system is uniquely solvable. If it were not, there would exist a nontrivial solution $\gamma^{(k)}$, $k = 0,\dots,\mathcal{N}_\varepsilon - 1$, of the homogeneous system

$$\sum_{k=0}^{\mathcal{N}_\varepsilon-1} \gamma^{(k)}\,A_n^-(0;\boldsymbol{w}_\alpha^{(k)}) = 0,\ n = 0,\dots,\mathcal{N}_\varepsilon - 1.$$

Consider then the field $(\boldsymbol{w}, \boldsymbol{w}_\alpha)$ given by

$$\boldsymbol{w} = \sum_{k=0}^{\mathcal{N}_\varepsilon - 1} \gamma^{(k)}\, \boldsymbol{w}^{(k)},\ \boldsymbol{w}_\alpha = \sum_{k=0}^{\mathcal{N}_\varepsilon - 1} \gamma^{(k)}\, \left(\boldsymbol{w}_\alpha^{(k)} - \boldsymbol{u}_{k,\alpha} \right).$$

It is easy to check, again by linearity, that $(\boldsymbol{w}, \boldsymbol{w}_\alpha)$ is a solution to problem (19)-(20)-(21) with $\boldsymbol{f} = \boldsymbol{0}$ and $\boldsymbol{u}_{\rm inc} = \boldsymbol{0}$. This last problem being well-posed, we must have $(\boldsymbol{w}, \boldsymbol{w}_\alpha) = (\boldsymbol{0}, \boldsymbol{0})$. It then follows from the linear independance of the auxiliary fields that $\gamma^{(k)} = 0$, $k = 0, \ldots, \mathcal{N}_\varepsilon - 1$, which contradicts the supposition. □

Remark 2. *Let us emphasize that the possible exponential growth of the solution, due to the presence of backward propagating modes, is taken into account by the fields $\boldsymbol{u}_{k,\alpha}$, through their dependence with respect to the axial variable which is analytically known (see* (22)*). All the other terms involved remain bounded in the computational domain, including the PML. As a consequence, in our approach, the exponential behavior of the solution does not raise any numerical issue.*

Note that the assumption of well-posedness in lemma 1 is not an unrealistic one, as we conjecture, using perturbation theory and the fact that the original problem (10) is well-posed, that it is satisfied for any sufficiently small value of the tolerance ε.

Also, the auxiliary fields used to "correct" $(\widetilde{\boldsymbol{u}}^L, \widetilde{\boldsymbol{u}}_\alpha^L)$ may be defined differently. Observe that they satisfy a series of problems which are very similar to problem (15). The rationale behind these specific choices will be made clear in the next section.

5 Practical implementation

Let us give some details regarding the proper implementation of the proposed method of solution using a finite element approach. Note that other discretization techniques, like finite differences for instance, could certainly be worked out, albeit differently since much of the present exposition relies on a weak formulation of the problem.

First, it can be shown that the solution to (15) satisfies the following weak formulation of the problem: *find* $(\boldsymbol{u}^L, \boldsymbol{u}_\alpha^L)$ *in* $H^1(\Omega_0)^d \times H^1(\Omega_+^L)^d$*, such that* $\boldsymbol{u}^L - \boldsymbol{u}_{\rm inc} = \boldsymbol{u}_\alpha^L$ *on* Σ_+ *and, for all* $\boldsymbol{v}$ *in* $H^1(\Omega_L)^d$*,*

$$\int_{\Omega_0} \left(-\rho\,\omega^2\, \boldsymbol{u}^L \cdot \overline{\boldsymbol{v}} + \boldsymbol{\sigma}(\boldsymbol{u}^L) : \boldsymbol{\nabla} \overline{\boldsymbol{v}} \right) \mathrm{d}\boldsymbol{x} + \int_{\Omega_+^L} \frac{1}{\alpha} \left(-\rho\,\omega^2\, \boldsymbol{u}_\alpha^L \cdot \overline{\boldsymbol{v}} + \boldsymbol{\sigma}_\alpha(\boldsymbol{u}_\alpha^L) : \boldsymbol{\nabla}_\alpha \overline{\boldsymbol{v}} \right) \mathrm{d}\boldsymbol{x}$$
$$= \int_{\Omega_0} \boldsymbol{f} \cdot \overline{\boldsymbol{v}}\, \mathrm{d}\boldsymbol{x} + \int_{\Sigma_+} \boldsymbol{\sigma}(\boldsymbol{u}_{\rm inc}) \boldsymbol{n} \cdot \overline{\boldsymbol{v}}\, \mathrm{d}\sigma. \quad (25)$$

Likewise, the auxiliary fields $(\boldsymbol{w}^{(k)}, \boldsymbol{w}_\alpha^{(k)})$, $k = 0, \ldots, \mathcal{N}_\varepsilon - 1$, satisfy: *find* $(\boldsymbol{w}_\alpha, \boldsymbol{w}_\alpha^{(k)})$ *in* $H^1(\Omega_0)^d \times H^1(\Omega_+^L)^d$*, such that* $\boldsymbol{w}^{(k)} = \boldsymbol{w}_\alpha^{(k)} - \boldsymbol{u}_{k,\alpha}$ *on* Σ_+ *and, for all* $\boldsymbol{v}$ *in* $H^1(\Omega_L)^d$*,*

$$\int_{\Omega_0} \left(-\rho\,\omega^2\, \boldsymbol{w}^{(k)} \cdot \overline{\boldsymbol{v}} + \boldsymbol{\sigma}(\boldsymbol{w}^{(k)}) : \boldsymbol{\nabla} \overline{\boldsymbol{v}} \right) \mathrm{d}\boldsymbol{x} + \int_{\Omega_+^L} \frac{1}{\alpha} \left(-\rho\,\omega^2\, \boldsymbol{w}_\alpha^{(k)} \cdot \overline{\boldsymbol{v}} + \boldsymbol{\sigma}_\alpha(\boldsymbol{w}_\alpha^{(k)}) : \boldsymbol{\nabla}_\alpha \overline{\boldsymbol{v}} \right) \mathrm{d}\boldsymbol{x}$$
$$= - \int_{\Sigma_+} \boldsymbol{\sigma}_\alpha(\boldsymbol{u}_{k,\alpha}) \boldsymbol{n} \cdot \overline{\boldsymbol{v}}\, \mathrm{d}\sigma. \quad (26)$$

The data for the last series of problems are guided modes, which are in general not known explicitly. In the case of Rayleigh–Lamb modes, a closed-form expression of the displacement field can be used, provided that the associated wavenumbers, which are the zeros of a transcendental equation (see Figure 2), are known. The determination of these can therefore be achieved with an excellent numerical accuracy(that is, within machine precision) by solving a discretized linear eigenproblem, followed by a refining process using the Newton–Raphson rootfinding method (see [31]). In the general three-dimensional case, one can use the SAFE method mentioned in subsection 2.2 to obtain numerical approximations of the wavenumbers and displacement fields characterizing the modes of the guide. Note that only the knowledge of the first $\mathcal{N}_\varepsilon$ modes (those inducing a failure of the PML method with respect to the prescribed tolerance ε) is needed.

Once these quantities are available, problems (25) and (26) can be discretized, using a conforming finite element space defined over a mesh of the domain Ω^L, and subsequently solved, leading to finite element approximations of the quantities $\boldsymbol{u}^L$ and $\boldsymbol{w}^{(k)}$. It should be remarked that the computation of these various numerical approximations

is not as costly as one would expect at first. Indeed, the structure of problems (25) and (26) being identical, the algebraic systems associated with their discrete counterparts share the same (sparse) matrix and differ only by their respective right-hand sides. As a consequence, once the former has been factorized, obtaining the approximations merely amounts to a succession of assemblies of the latter, followed by forward and backward substitutions.

The effective construction of the approximation $\widetilde{\boldsymbol{u}}^L$ according to (23) next entails the determination of the coefficients $\mu^{(k)}$, $k = 0, \ldots, \mathcal{N}_\varepsilon - 1$, knowing that these are solution to the linear system (24). To compute the entries of the matrix (resp. right-hand side vector) of this system, one needs to exploit the biorthogonality relations, which requires to have access to the approximations of the quantities $X(\boldsymbol{w}_\alpha^L)$ and $Y(\boldsymbol{w}_\alpha^L)$ (resp. $X(\boldsymbol{u}_\alpha^L)$ and $Y(\boldsymbol{u}_\alpha^L)$) on a given cross-section of the bounded domain. Note that it is an easy task to retrieve at no cost the values of an approximation to $\boldsymbol{u}_\alpha^L$ and $\boldsymbol{w}_\alpha^L$ on a cross-section from their computed finite element approximations as long as this section is part the mesh boundary and Lagrange finite elements (whose degrees of freedom are attached to nodes of the simplices constituting the mesh) are used. For this reason, it is particularly convenient to choose the cross-section as the interface Σ_+ between the domains Ω_0 and Ω_+^L. On the contrary, obtaining approximations to $\boldsymbol{t}_s(\boldsymbol{w}_\alpha^L)$ and $t_d(\boldsymbol{w}_\alpha^L)$ (resp. $\boldsymbol{t}_s(\boldsymbol{u}_\alpha^L)$ and $t_d(\boldsymbol{u}_\alpha^L)$) on the same interface, that is recovering values of $\boldsymbol{\sigma}(\boldsymbol{w}_\alpha^L)\boldsymbol{n}$ (resp. $\boldsymbol{\sigma}(\boldsymbol{u}_\alpha^L)\boldsymbol{n}$) since $\boldsymbol{n} = \boldsymbol{e}_d$ on a cross-section, is not so straightforward and implies some additional post-processing (see [32]). Indeed, it follows from the Green formula that the restriction $\boldsymbol{u}_\alpha^L$ satisfies

$$\int_{\Omega_+^L} \frac{1}{\alpha} \left(-\rho\omega^2\, \boldsymbol{u}_\alpha^L \cdot \overline{\boldsymbol{v}} + \lambda\, \mathrm{div}_\alpha(\boldsymbol{u}_\alpha^L)\, \mathrm{div}_\alpha(\overline{\boldsymbol{v}}) + 2\mu\, \boldsymbol{\varepsilon}_\alpha(\boldsymbol{u}_\alpha^L) : \boldsymbol{\varepsilon}_\alpha(\overline{\boldsymbol{v}}) - \boldsymbol{f} \cdot \overline{\boldsymbol{v}} \right) \mathrm{d}\boldsymbol{x}$$
$$= \int_{\partial\Omega_+^L} \frac{1}{\alpha} \left(\boldsymbol{\sigma}_\alpha(\boldsymbol{u}_\alpha^L)\boldsymbol{n} \right) \cdot \overline{\boldsymbol{v}}\, \mathrm{d}\sigma,\ \forall \boldsymbol{v} \in H^1(\Omega_+^L)^d.$$

The discrete analogue of this equality allows one, by selecting the test functions to be the basis functions which have degrees of freedom with support located on Σ_+, to obtain the desired values, at the expense of solving a (small) linear system. It then remains to assemble and solve the system (24) of size $\mathcal{N}_\varepsilon$ to obtain the desired numerical approximation.

In any case, in order to evaluate the various products appearing in the expression of the modal coefficients, the quantities $\mathbf{X}_k$ and $\mathbf{Y}_k$, $k = 0, \ldots, \mathcal{N}_\varepsilon - 1$, associated with the guided modes are discretized in the finite element basis and the same quadrature formulas as for the rest of the finite element part of the computations are used.

We may therefore summarize the implementation of the method into the following successive steps.

(1) Computation of a numerical approximation of the solution to problem (25).

(2) Determination of the $\mathcal{N}_\varepsilon$ modes responsible for the PML failure.

(3) Computation of numerical approximations of the auxiliary fields satisfying the family of problems (26).

(4) Post-processing of the computed fields in order to exploit the biorthogonality relations and obtain the entries of the linear system (24).

(5) Calculation of the coefficients $\mu^{(k)}$, $k = 0, \ldots, \mathcal{N}_\varepsilon - 1$, by solving (24) and construction of the corrected approximate solution according to (23).

We emphasize that all of the above involve computations which are quite standard for any familiar user of finite element codes or libraries, allowing the method to be implemented with little programming effort. Besides, one may also remark that step 2 is unrelated to step 1, and that the problems solved in step 3, while sharing some common traits with (25) as explained above, are independent of the data $\boldsymbol{f}$ and $\boldsymbol{u}_{\mathrm{inc}}$ for the problem solved in the first step. Therefore, if the geometry of the waveguide and the pulsation ω, as well as the discretization, are fixed, one can precompute, during an "offline" phase (as in model reduction techniques such as reduced basis approximation), the auxiliary fields once and for all, a parallel implementation being straightforward. The matrix of the linear system (24) for the coefficients of the correction can even be assembled and factorized, leaving to the "online" phase the assembly of the right-hand side of the linear system for every given set of data. The method is thus particularly efficient when used in such a context, since a major part of its supplementary cost can be factored out of each time it is applied.

We should also add that, compared to the approach of Skelton *et al.* in [8], which involves at least two different PML coefficients (one for the forward propagating modes and one for the backward (or long) ones), our procedure is only a corrective post-processing of the solution obtained using the PML technique in a classical way.

We conclude this section by discussing the extension of the method to the case of an infinite waveguide. In that case, let Ω denote the waveguide, the bounded domain Ω_0, presenting variations of the cross section and/or enclosing the defects and sources, being defined by $\Omega_0 = \Omega \cap \{(\boldsymbol{x}_S, x_d) \,|\, -l < x_d < l\}$, with $l > 0$, and the two perfectly matched layers being $\Omega_+^L = S \times [l, l+L]$ and $\Omega_-^L = S \times [-l-L, -l]$, with respective interfaces Σ_+ and Σ_- and back ends Σ_+^L and Σ_-^L. As two layers are present in this problem, one has to double the number of auxiliary fields used to correct the PML solution accordingly. We hence introduce two families $(\boldsymbol{w}_+^{(k)}, \boldsymbol{w}_{+,\alpha}^{(k)})$ and $(\boldsymbol{w}_-^{(k)}, \boldsymbol{w}_{-,\alpha}^{(k)})$, $k = 0, \ldots, \mathcal{N}_\varepsilon - 1$, which are respectively solutions to

$$
\begin{aligned}
&-\rho\omega^2 \boldsymbol{w}_+^{(k)} - \mathrm{div}(\boldsymbol{\sigma}(\boldsymbol{w}_+^{(k)})) = \boldsymbol{0} \text{ in } \Omega_0,\\
&-\rho\omega^2 \boldsymbol{w}_{+,\alpha}^{(k)} - \mathrm{div}_\alpha(\boldsymbol{\sigma}_\alpha(\boldsymbol{w}_{+,\alpha}^{(k)})) = \boldsymbol{0} \text{ in } \Omega_+^L \cup \Omega_-^L,\\
&\boldsymbol{\sigma}(\boldsymbol{w}_+^{(k)})\boldsymbol{n} = \boldsymbol{0} \text{ on } \partial\Omega \cap \partial\Omega_0,\\
&\boldsymbol{\sigma}_\alpha(\boldsymbol{w}_{+,\alpha}^{(k)})\boldsymbol{n} = \boldsymbol{0} \text{ on } \partial\Omega \cap \partial(\Omega_+^L \cup \Omega_-^L),\\
&\boldsymbol{w}_+^{(k)} = \boldsymbol{w}_{+,\alpha}^{(k)} - \boldsymbol{u}_{k,\alpha},\ \boldsymbol{\sigma}_\alpha(\boldsymbol{w}_+^{(k)})\boldsymbol{n} = \boldsymbol{\sigma}_\alpha(\boldsymbol{w}_{+,\alpha}^{(k)} - \boldsymbol{u}_{k,\alpha}^+)\boldsymbol{n} \text{ on } \Sigma_+,\\
&\boldsymbol{w}_+^{(k)} = \boldsymbol{w}_{+,\alpha}^{(k)},\ \boldsymbol{\sigma}_\alpha(\boldsymbol{w}_+^{(k)})\boldsymbol{n} = \boldsymbol{\sigma}_\alpha(\boldsymbol{w}_{+,\alpha}^{(k)})\boldsymbol{n} \text{ on } \Sigma_-,\\
&(\boldsymbol{w}_{+,\alpha}^{(k)})_S = \boldsymbol{0},\ t_{\alpha d}(\boldsymbol{w}_{+,\alpha}^{(k)}) = 0 \text{ on } \Sigma_+^L \cup \Sigma_-^L,
\end{aligned}
$$

and

$$
\begin{aligned}
&-\rho\omega^2 \boldsymbol{w}_-^{(k)} - \mathrm{div}(\boldsymbol{\sigma}(\boldsymbol{w}_-^{(k)})) = \boldsymbol{0} \text{ in } \Omega_0,\\
&-\rho\omega^2 \boldsymbol{w}_{-,\alpha}^{(k)} - \mathrm{div}_\alpha(\boldsymbol{\sigma}_\alpha(\boldsymbol{w}_{-,\alpha}^{(k)})) = \boldsymbol{0} \text{ in } \Omega_+^L \cup \Omega_-^L,\\
&\boldsymbol{\sigma}(\boldsymbol{w}_-^{(k)})\boldsymbol{n} = \boldsymbol{0} \text{ on } \partial\Omega \cap \partial\Omega_0,\\
&\boldsymbol{\sigma}_\alpha(\boldsymbol{w}_{-,\alpha}^{(k)})\boldsymbol{n} = \boldsymbol{0} \text{ on } \partial\Omega \cap \partial(\Omega_+^L \cup \Omega_-^L),\\
&\boldsymbol{w}_-^{(k)} = \boldsymbol{w}_{-,\alpha}^{(k)},\ \boldsymbol{\sigma}_\alpha(\boldsymbol{w}_-^{(k)})\boldsymbol{n} = \boldsymbol{\sigma}_\alpha(\boldsymbol{w}_{-,\alpha}^{(k)})\boldsymbol{n} \text{ on } \Sigma_+,\\
&\boldsymbol{w}_-^{(k)} = \boldsymbol{w}_{-,\alpha}^{(k)} - \boldsymbol{u}_{k,\alpha},\ \boldsymbol{\sigma}_\alpha(\boldsymbol{w}_-^{(k)})\boldsymbol{n} = \boldsymbol{\sigma}_\alpha(\boldsymbol{w}_{-,\alpha}^{(k)} - \boldsymbol{u}_{k,\alpha}^-)\boldsymbol{n} \text{ on } \Sigma_-,\\
&(\boldsymbol{w}_{-,\alpha}^{(k)})_S = \boldsymbol{0},\ t_{\alpha d}(\boldsymbol{w}_{-,\alpha}^{(k)}) = 0 \text{ on } \Sigma_+^L \cup \Sigma_-^L,
\end{aligned}
$$

the approximate solution $\widetilde{\boldsymbol{u}}^L$ in Ω_0 now being defined by

$$
\widetilde{\boldsymbol{u}}^L = \boldsymbol{u}^L + \sum_{k=0}^{\mathcal{N}_\varepsilon - 1} \left(\mu_+^{(k)}\, \boldsymbol{w}_+^{(k)} + \mu_-^{(k)}\, \boldsymbol{w}_-^{(k)} \right),
$$

where the sets of coefficients $\mu_+^{(k)}$ and $\mu_-^{(k)}$, $k = 0, \ldots, \mathcal{N}_\varepsilon - 1$, verify the relations

$$
A_n^-(l; \boldsymbol{u}_\alpha^L) + \sum_{k=0}^{\mathcal{N}_\varepsilon - 1} \left(\mu_+^{(k)}\, A_n^-(l; \boldsymbol{w}_{+,\alpha}^{(k)}) + \mu_-^{(k)}\, A_n^-(l; \boldsymbol{w}_{-,\alpha}^{(k)}) \right) = 0,\ n = 0, \ldots, \mathcal{N}_\varepsilon - 1,
$$

$$
A_n^+(-l; \boldsymbol{u}_\alpha^L) + \sum_{k=0}^{\mathcal{N}_\varepsilon - 1} \left(\mu_+^{(k)}\, A_n^+(-l; \boldsymbol{w}_{+,\alpha}^{(k)}) + \mu_-^{(k)}\, A_n^+(-l; \boldsymbol{w}_{-,\alpha}^{(k)}) \right) = 0,\ n = 0, \ldots, \mathcal{N}_\varepsilon - 1,
$$

and are thus obtained by solving a block-diagonal linear system of size $2\,\mathcal{N}_\varepsilon$.

6 Numerical results

We present a few numerical results to validate the new method and assert its pertinence for the computation of solutions in a two-dimensional (infinite) plate by comparing it to a reference solution, which either has a closed form or is obtained numerically using a finite element method and the extension of the Dirichlet-to-Neumann approach proposed in [14]. In these numerical experiments, the values $\rho = 2700$ kg m^{-1} for the mass density, $E = 69$ GPa for the Young modulus and $\nu = 0.33$ for the Poisson ration are used, corresponding to a plate made of aluminium. The plate itself has thickness $2h$, with $h = 1$ m. In each of the simulations, we used the homogeneous boundary condition advocated in subsection 3.2 at the end of the layers. Other choices of conditions, like a homogeneous Dirichlet condition (i.e., $\boldsymbol{u}_\alpha^L = \boldsymbol{0}$ on $\Sigma_+^L \cup \Sigma_-^L$) or a homogeneous Neumann condition (i.e., $\boldsymbol{\sigma}_\alpha(\boldsymbol{u}_\alpha^L)\boldsymbol{n} = \boldsymbol{0}$ on $\Sigma_+^L \cup \Sigma_-^L$), have been shown to produce quantitatively and qualitatively similar results.

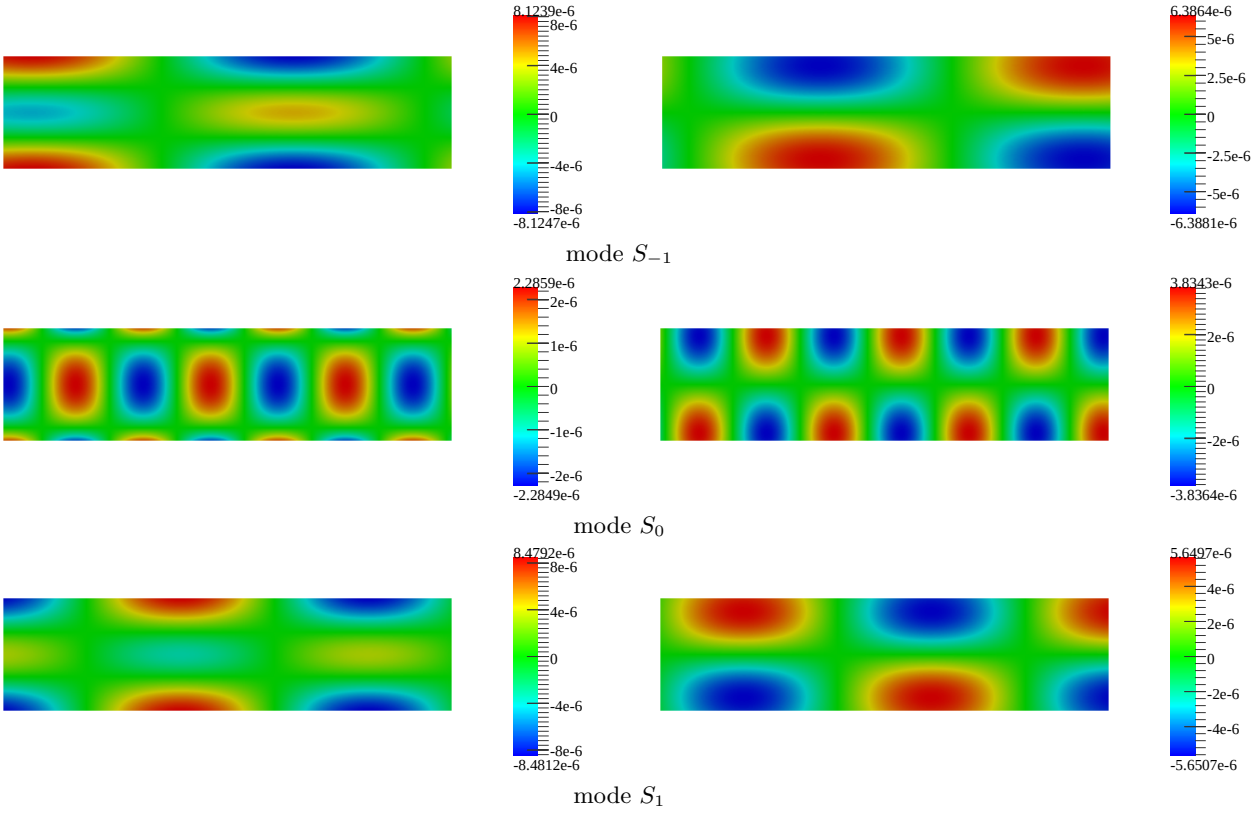

Figure 4: Real parts of the horizontal (on the left) and vertical (on the right) components of the symmetric propagative Rayleigh–Lamb modes for $\omega = 8833.7825\ \mathrm{rad\,s^{-1}}$ in a plate of thickness 2 m made of aluminium.

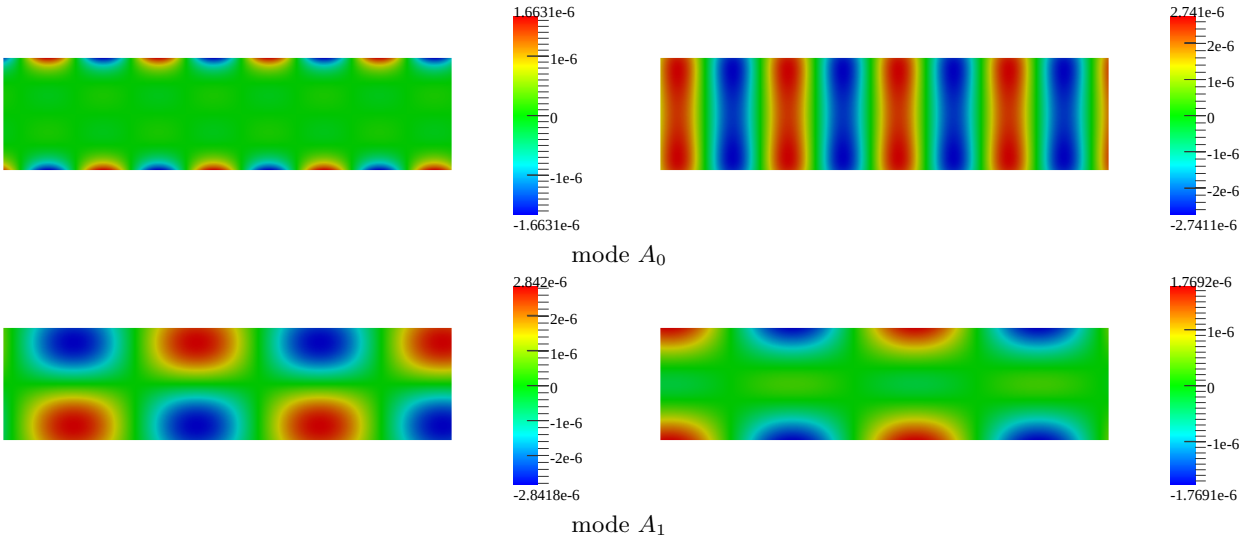

Figure 5: Real parts of the horizontal (on the left) and vertical (on the right) components of the antisymmetric propagative Rayleigh–Lamb modes for $\omega = 8833.7825$ rad s^{-1} in a plate of thickness 2 m made of aluminium.

We first consider the case of an incoming wave composed of a combination of propagative guided modes, one of them being backward. For $\omega = 8833.7825$ rad s^{-1} (which corresponds to $\tilde{\omega} = 2.85$, see Figure 2), there exist five propagative guided modes, associated with the first four dispersion curves in Figure 2, three symmetric ones (see Figure 4) with respective wavenumbers (in m^{-1}) $\beta = -0.66995$ (corresponding to a backward propagating mode, which we denote by S_{-1} in what follows), $\beta = 0.93833$ (mode S_0) and $\beta = 2.61386$ (mode S_1), and two antisymmetric ones (see Figure 5) with respective wavenumbers (in m^{-1}) $\beta = 1.43166$ (mode A_0) and $\beta = 3.19204$ (mode A_1), all of which are indexed in this order. The incident wave is chosen as the sum of the symmetric propagative modes. The length of the domain Ω_0 is 4 m (that is $l = 2$ m), while that of the two layers bounding the computational domain is $L = 0.5$ m. The argument of the complex parameter α, held constant throughout the computations, is equal to $-\frac{\pi}{4}$. Finally, a nonstructured mesh of the domain Ω^L, made of triangles of size 0.05 m, and Lagrange finite elements of second order are used for the finite element computation, giving about 15 discretization points per wavelength in the domain Ω_0.

The Figure 6 shows, in a semi-logarithmic plot, the relative error on the computed solution measured in the discrete $H^1(\Omega_0)$ norm for the classical PML method (curve for $\mathcal{N}_\varepsilon = 0$) and the novel approach (other curves) as a function of the modulus of α. As expected, we observe that, due to the presence of a backward mode, the error for the PML method is more or less constant instead of exponentially decrease as $|\alpha|$ tends to zero. Taking into account the mode S_{-1} via the new approach (curve $\mathcal{N}_\varepsilon = 1$) suffices to retrieve the usual behavior of the method error: the error diminishes with $|\alpha|$ up to a minimal value and then increases dramatically as the finite element discretization is unable to properly resolve the highly decreasing and oscillating solution in the PML. Choosing an adequate value for $|\alpha|$ then allows to compute an accurate approximate solution, with a relative error of less than a percent. If other propagative modes are added to the post-processing (see the subsequent curves for $\mathcal{N}_\varepsilon = 2$ to 5, the modes being added as follows: first S_{-1}, then S_0, S_1, A_0 and finally A_1), the minimal value can be further decreased, until all the propagative modes in the solution have been exhausted (indeed, the last three error curves, that is for $\mathcal{N}_\varepsilon = 3$ to 5, are indiscernible, which means that the addition of the odd modes does not improve the approximation), at which point the error of the method is virtually independent of the value of $|\alpha|$ and stagnates at a level which we interpret[4] as the discretization error for the tested case.

When a long mode is present, the situation is different, since the PML method produces a solution that converges to the exact one as $|\alpha|$ tends to zero. Still, this convergence is very slow and our approach is thus relevant. For $\omega = 9738.2379$ rad s^{-1} (which corresponds to $\tilde{\omega} = 3.1418$), there are five propagative guided modes, associated with the first five dispersion curves in Figure 2, three of which are symmetric, with respective wavenumbers (in m^{-1}) $\beta = 0.00344$ (mode S_0), $\beta = 1.43706$ (mode S_1) and $\beta = 3.04091$ (mode S_2), and two are antisymmetric, with respective wavenumbers (in m^{-1}) $\beta = 1.68301$ (mode A_0) and $\beta = 3.48928$ (mode A_1). As before, the sum of the

[4]Using some finer (resp. coarser) meshes, we observed lower (resp. higher) levels of error which are consistent with the convergence rate of the finite elements used for the experiments.

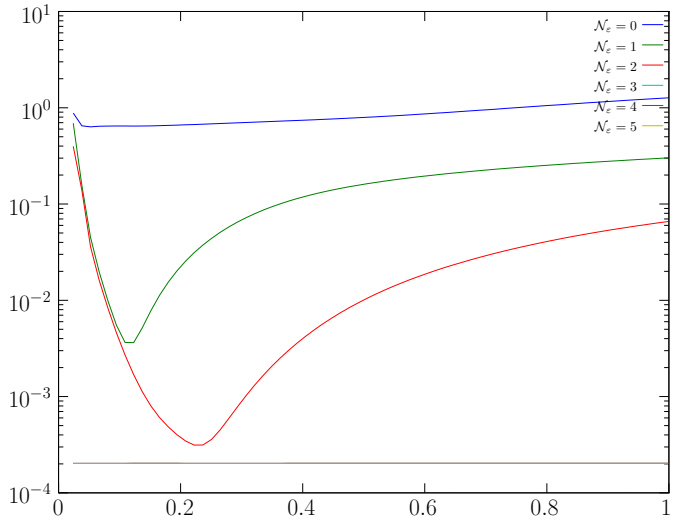

Figure 6: Relative error in $H^1(\Omega_0)^2$ norm as a function of $|\alpha|$ when a backward propagating mode is present. The case $\mathcal{N}_\varepsilon = 0$ corresponds to the classical PML method.

propagative symmetric modes is used as the incident wave and the same finite element discretization is employed, meaning that about 13 discretization points per wavelength are used in the domain Ω_0 for this simulation.

We see on the Figure 7 that the discretization chosen here does not allow for a clear observation of the very slow rate of convergence of the PML method in this case. Nevertheless, an improvement appears as soon as the long mode is taken into account with the new approach. As before, we also see that the method performs better when more modes are incorporated into the post-processing.

A second and more qualitative numerical experiment deals with the case of a perturbed waveguide, for which a closed form solution is, *a priori*, not available. The numerical solutions produced the PML method and the novel approach are thus compared with an approximation obtained by using a similar finite element discretization and the transparent boundary conditions developed in [14]. The configuration is identical to that of the first of the previous simulations, except for the plate, which is now locally perturbed by a single rectangular slot. The incident wave is the sum of the five (symmetric and antisymmetric) propagative modes and the PML parameter α has value $0.065(1 - \mathrm{i})$. The real parts of both components of the reference solution for this scattering problem are presented on Figure 8, while the real parts of the components of the PML and post-processed numerical solutions (with $\mathcal{N}_\epsilon = 5$) are respectively given in Figures 9 and 10. There is a perfect agreement between the numerical solutions computed respectively by the former and the latter methods, with a relative difference in $H^1(\Omega_0)^2$ norm equal to 3.45×10^{-3}. On the contrary, we notice a large discrepancy, which is confirmed by a relative difference in $H^1(\Omega_0)^2$ norm equal to 3.4824, between the approximation obtained with the PML method alone and these two solutions.

7 Some open mathematical questions

The method we proposed in this paper depends on several theoretical statements that are now discussed.

First, we extensively used modal decompositions of the elastic field in straight parts of the waveguide, and the existence of such expansions is not obvious. Indeed, contrary to the simple scalar case (Helmholtz equation with Dirichlet or Neumann boundary conditions), the eigenproblem for the modes is not selfadjoint, and, as a consequence, there is no result ensuring that the family of modes forms a basis in some space of vectorial functions of the variable $\boldsymbol{x}_S$. However, we think this shortcoming could be overcome by using the theory presented in [33, chapter 5, paragraph 7] for the static case, which instead rely on the use of the Fourier transform in the axial direction of the guide together with Cauchy's residue theorem for analytic functions. This approach is quite intricate and exposing it is clearly beyond the scope of this article.

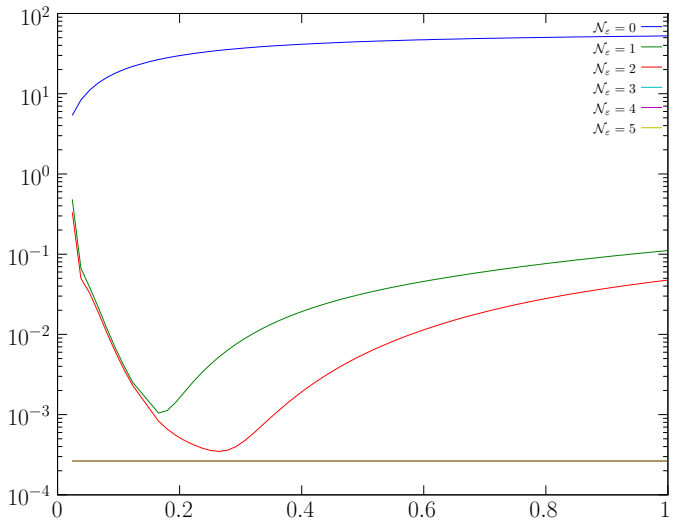

Figure 7: Relative error in $H^1(\Omega_0)^2$ norm as a function of $|\alpha|$ when a long propagative mode is present. The case $\mathcal{N}_\varepsilon = 0$ corresponds to the classical PML method.

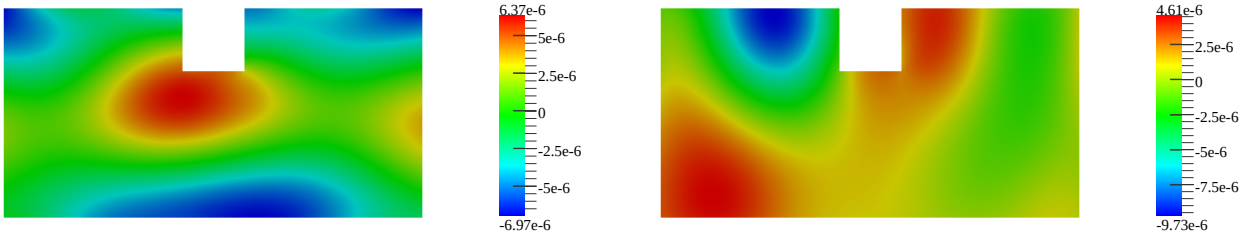

Figure 8: Real parts of the horizontal (on the left) and vertical (on the right) components of the reference solution computed using transparent boundary conditions (see [14]).

Second, let us discuss assumption 3, which supposes the well-posedness of problem (15). When the PML coefficient α is a real number, we can show that this problem is of Fredholm type using Korn's second inequality. By a continuity argument, one may infer this is still the case with α taking complex values near the real axis, that is when $\arg(\alpha)$ is small. However, such a restriction does not seem to be necessary in practice and the numerical method typically works for the choice $\arg(\alpha) = -\frac{\pi}{4}$. We tried to find an explicit bound on the argument of α by deriving a Korn-like inequality. Unfortunately, while such an inequality can be easily established for the PML problem with a Dirichlet boundary condition, we did not succeed in proving a similar result in the present setting using classical techniques (see [34] for instance). The difficulty here comes from the combination of the free-surface boundary condition and the complex coefficients, depending on the parameter α, of the underlying differential operator.

Once the Fredholm nature of problem (15) has been established, proving its well-posedness still requires a uniqueness result. Using compactness arguments, one can prove that the set of values of ω for which uniqueness of the solution to (15) does not hold is discrete. One must then distinguish two cases, depending on the existence or not of backward propagating modes.

- Without backward propagating modes and using the mathematical tools in [33] mentioned above, we should be able to prove that problem (15) is well-posed for L large enough, its solution converging as L tends to infinity to the solution of the initial problem (10), which is itself well-posed in virtue of assumption 2 (saying that there is no trapped mode at the considered frequency).

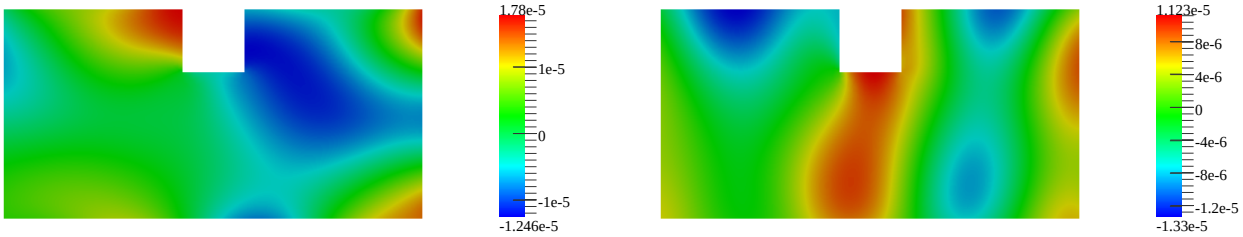

Figure 9: Real parts of the horizontal (on the left) and vertical (on the right) components of the solution computed using perfectly matched layers.

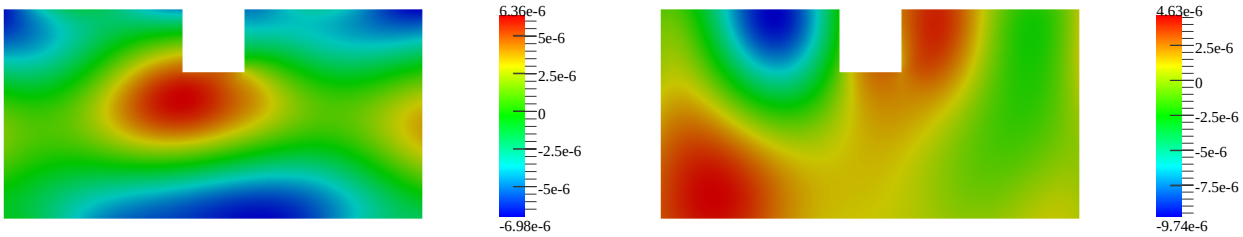

Figure 10: Real parts of the horizontal (on the left) and vertical (on the right) components of the reference solution computed using perfectly matched layers and the novel approach with $\mathcal{N}_\epsilon = 5$.

- In the presence of backward propagating modes, the situation is more complex. Indeed, in this case, the solution to problem (15) (if it exists) will converge as L tends to infinity to the solution of a problem in which the difference $\boldsymbol{u} - \boldsymbol{u}_{\text{inc}}$ is no longer a superposition of rightgoing modes, but of modes with a positive phase velocity. To prove the well-posedness of problem (15) for L large enough, we need this nonphysical limit problem to be well-posed. Now, it can be shown this problem is ill-posed (in the sense that uniqueness does not hold) not only when assumption 2 does not hold (that is when trapped modes exist), but also when an incident backward propagating mode is totally converted into other modes. This can occur for some particular frequencies and it would be interesting to test the method near such values.

References

[1] J.-P. Bérenger, A perfectly matched layer for the absorption of electromagnetic waves, J. Comput. Phys. 114 (2) (1994) 185–200. doi:10.1006/jcph.1994.1159.

[2] D. Rabinovich, D. Givoli, E. Bécache, Comparison of high-order absorbing boundary conditions and perfectly matched layers in the frequency domain, Internat. J. Numer. Methods Biomed. Engrg. 26 (10) (2010) 1351–1369. doi:10.1002/cnm.1394.

[3] E. Bécache, S. Fauqueux, P. Joly, Stability of perfectly matched layers, group velocities and anisotropic waves, J. Comput. Phys. 188 (2) (2003) 399–433. doi:10.1016/S0021-9991(03)00184-0.

[4] H. Lamb, On group-velocity, Proc. London Math. Soc. (2) 1 (1) (1904) 473–479. doi:10.1112/plms/s2-1.1.473.

[5] A. H. Meitzler, Wave propagation in elastic plates: low and high mode dispersion, J. Acoust. Soc. Am. 38 (5) (1965) 835–842. doi:10.1121/1.1908675.

[6] P. J. B. Clarricoats, R. A. Waldron, Non-periodic slow-wave and backward-wave structures, J. Electron. Control 8 (6) (1960) 455–458. doi:10.1080/00207216008937291.

[7] A. A. Maznev, A. G. Every, Existence of backward propagating acoustic waves in supported layers, Wave Motion 48 (5) (2011) 401–407. doi:10.1016/j.wavemoti.2011.02.002.

[8] E. A. Skelton, S. D. Adams, R. V. Craster, Guided elastic waves and perfectly matched layers, Wave Motion 44 (7-8) (2007) 573–592. doi:10.1016/j.wavemoti.2007.03.001.

[9] P.-R. Loh, A. F. Oskooi, M. Ibanescu, M. Skorobogatiy, S. G. Johnson, Fundamental relation between phase and group velocity, and application to the failure of perfectly matched layers in backward-wave structures, Phys. Rev. E 79 (6) (2009) 065601–1–4. doi:10.1103/PhysRevE.79.065601.

[10] A.-S. Bonnet-Ben Dhia, G. Legendre, An alternative to Dirichlet-to-Neumann maps for waveguides, C. R. Acad. Sci. Paris Sér. I Math. 349 (17-18) (2011) 1005–1009. doi:10.1016/j.crma.2011.08.006.

[11] A. Barnett, L. Greengard, A new integral representation for quasi-periodic scattering problems in two dimensions, BIT 51 (1) (2011) 67–90. doi:10.1007/s10543-010-0297-x.

[12] R. B. Nelson, S. B. Dong, R. D. Kalra, Vibrations and waves in laminated orthotropic circular cylinders, J. Sound Vibration 18 (3) (1971) 429–444. doi:10.1016/0022-460X(71)90714-0.

[13] S. B. Dong, R. B. Nelson, On natural vibrations and waves in laminated orthotropic plates, J. Appl. Mech. 39 (3) (1972) 739–745. doi:10.1115/1.3422782.

[14] V. Baronian, A.-S. Bonnet-Ben Dhia, E. Lunéville, Transparent boundary conditions for the harmonic diffraction problem in an elastic waveguide, J. Comput. Appl. Math. 234 (6) (2010) 1945–1952. doi:10.1016/j.cam.2009.08.045.

[15] V. Pagneux, A. Maurel, Scattering matrix properties with evanescent modes for waveguides in fluids and solids, J. Acoust. Soc. Am. 116 (4) (2004) 1913–1920. doi:10.1121/1.1786293.

[16] V. Pagneux, A. Maurel, Lamb wave propagation in elastic waveguides with variable thickness, Proc. R. Soc. Lond. A 462 (2068) (2006) 1315–1339. doi:10.1098/rspa.2005.1612.

[17] W. B. Fraser, Orthogonality relation for the Rayleigh-Lamb modes of vibration of a plate, J. Acoust. Soc. Amer. 59 (1) (1976) 215–216. doi:10.1121/1.380851.

[18] L. G. Merkulov, S. I. Rokhlin, O. P. Zobnin, Calculation of the spectrum of wave numbers for Lamb waves in a plate, Soviet J. Nondestructive Testing 6 (1970) 369–373.

[19] V. Pagneux, Complex resonance and localized vibrations at the edge of a semi-infinite elastic cylinder, Math. Mech. Solids 17 (1) (2012) 17–26. doi:10.1177/1081286511412439.

[20] W. J. Zhou, M. N. Ichchou, J. M. Mencik, Analysis of wave propagation in cylindrical pipes with local inhomogeneities, J. Sound Vibration 319 (1-2) (2009) 335–354. doi:10.1016/j.jsv.2008.05.039.

[21] F. Benmeddour, F. Treyssède, L. Laguerre, Numerical modeling of guided wave interaction with non-axisymmetric cracks in elastic cylinders, Int. J. Solids Structures 48 (5) (2011) 764–774. doi:10.1016/j.ijsolstr.2010.11.013.

[22] U. Basu, A. K. Chopra, Perfectly matched layers for time-harmonic elastodynamics of unbounded domains: theory and finite-element implementation, Comput. Methods Appl. Mech. Engrg. 192 (11-12) (2003) 1337–1375. doi:10.1016/S0045-7825(02)00642-4.

[23] I. Harari, U. Albocher, Studies of FE/PML for exterior problems of time-harmonic elastic waves, Comput. Methods Appl. Mech. Engrg 195 (29-32) (2006) 3854–3879. doi:10.1016/j.cma.2005.01.024.

[24] J. H. Bramble, J. E. Pasciak, D. Trenev, Analysis of a finite PML approximation to the three dimensional elastic wave scattering problem, Math. Comp. 79 (272) (2010) 2079–2101. doi:10.1090/S0025-5718-10-02355-0.

[25] A. Bermúdez, L. Hervella-Nieto, A. Prieto, R. Rodríguez, An optimal perfectly matched layer with unbounded absorbing function for time-harmonic acoustic scattering problems, J. Comput. Phys. 223 (2) (2007) 469–488. doi:10.1016/j.jcp.2006.09.018.

[26] W. C. Chew, W. H. Weedon, A 3D perfectly matched medium from modified Maxwell's equations with stretched coordinates, IEEE Microwave Opt. Technol. Lett. 7 (13) (1994) 599–604. doi:10.1002/mop.4650071304.

[27] C. M. Rappaport, Interpreting and improving the PML absorbing boundary condition using anisotropic lossy mapping of space, IEEE Trans. Magn. 32 (3) (1996) 968–974. doi:10.1109/20.497403.

[28] S. A. Cummer, Perfectly matched layer behavior in negative refractive index materials, IEEE Antennas Wireless Propag. Lett. 3 (1) (2004) 172–175. doi:10.1109/LAWP.2004.833710.

[29] X. T. Dong, X. S. Rao, Y. B. Gan, B. Guo, W. Y. Yin, Perfectly matched layer-absorbing boundary condition for left-handed materials, IEEE Microw. Wireless Compon. Lett. 14 (6) (2004) 301–303. doi:10.1109/LMWC.2004.827104.

[30] E. Bécache, A.-S. Bonnet-Ben Dhia, G. Legendre, Perfectly matched layers for the convected Helmholtz equation, SIAM J. Numer. Anal. 42 (1) (2004) 409–433. doi:10.1137/S0036142903420984.

[31] V. Pagneux, A. Maurel, Determination of Lamb mode eigenvalues, J. Acoust. Soc. Amer. 110 (3) (2001) 1307–1314. doi:10.1121/1.1391248.

[32] G. F. Carey, Derivative calculation from finite element solutions, Comput. Methods Appl. Mech. Engrg. 35 (1) (1982) 1–14. doi:10.1016/0045-7825(82)90029-9.

[33] S. Nazarov, B. A. Plamenevsky, Elliptic problems in domains with piecewise smooth boundaries, Vol. 13 of De Gruyter Expositions in Mathematics, De Gruyter, 1994.

[34] J. A. Nitsche, On Korn's second inequality, RAIRO Anal. Numér. 15 (3) (1981) 237–248.